

EVALUATING A NEW DRUG TO COMBAT ALZHEIMER'S DISEASE

Name: Siyabonga G. Sibiya

Student Number: 208510719

Submitted in partial fulfillment of the requirements for the Degree Master of Medical Science in Human Physiology, in the Discipline of Human Physiology, School of Laboratory Medicine and Medical Sciences, College of Health Sciences



**UNIVERSITY OF
KWAZULU-NATAL**

**INYUVESI
YAKWAZULU-NATALI**

Supervisor: Prof. W.M.U Daniels

Co-supervisor: Dr M.V Mabandla

DECLARATION

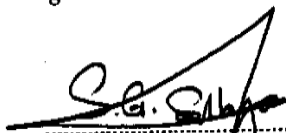
I, **Siyabonga Goodwill Sibiya** do hereby declare that all information provided in this thesis entitled:

“Evaluating a New Drug to Combat Alzheimer’s disease”

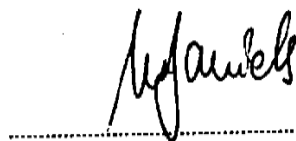
is the result of my own investigation and all the information taken from research papers is properly referenced. I understand that infringement or plagiarisms could lead to my degree being disqualified.

Signatures:

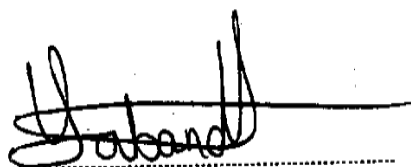
Date:


.....
Supervisee (S.G. Sibiya)

14 / 04 / 2015
.....


.....
Supervisor (Prof. W.M.U. Daniels)

14 / 4 / 15
.....


.....
Co-Supervisor (Dr. M.V. Mabandla)

14 / 04 / 2015
.....

ACKNOWLEDGEMENTS

To my supervisor Professor W.M.U Daniels and my co-supervisor Doctor M.V Mabandla, who have not only been supervisors, but also have played the role of a father(s) towards me. Their commitment to the advancement of science, constructive criticism, perseverance and encouragement has not only made me a better scientist, but has also taught me diverse ways of critically viewing a variety of other things around us as well. Thank you for sharing your wisdom with me Prof D and Dr M.

I would like to also thank Professor Vivienne Russell for all her valued scientific inputs which ensured that this thesis is completed and it contains knowledge that propels science forward and contributes positively to the already vast scientific knowledge that exists.

I would like to acknowledge Professor Thavi Govender and Professor Gert Kruger and their research team, Adeola Shobo and Sdu in particular, at the University of KwaZulu-Natal Catalysis and Peptide Research Unit for all their collaborative efforts, their enthusiasm towards the advancement of science as a whole and ensuring that this study was a success, thank you all.

I would like to acknowledge my colleagues who have always been there in all the experimental work that needed team work, even if it meant working long hours, and for the guidance that they have given to me through this journey, thanks guys.

I would finally like to acknowledge the National Research Foundation for their financial contributions towards this study.

I would not have made it this far without you all, may the Lord abundantly bless you all.

Thank you.



PRESENTATIONS

6th International Congress on Pharmaceutical and Pharmacological Sciences (ICPPS) - 2011

Presentation type: Poster presentation

The South African Society of Psychiatrists (SASOP) Biological Psychiatry Congress - 2013

Presentation type: Oral presentation and E-poster

Southern African Neurosciences Society (SANS) Symposium - 2014

Presentation type: Oral presentation

University of KwaZulu-Natal, School of Laboratory Medicines and Medical Sciences Research Symposium - 2014

Presentation type: Oral presentation

LIST OF ABBREVIATIONS

AA's	Amino acids
A β ₄₂ /A β	Amyloid- β protein
AD	Alzheimer's disease
ADAM	A disintegrin and metalloprotease domain
AICD	Amyloid Precursor Protein intracellular domain
APP	Amyloid Precursor Protein
BACE1	Beta site Amyloid Precursor Protein cleaving enzyme 1
BBB	Blood Brain Barrier
BSB	Beta Sheet Breaker
C3	Caspase 3
CTF	Carboxyl terminal fragment
DISC	Death inducing signaling complex
ELISA	Enzyme-linked Immunosorbent assay
ER	Endoplasmic reticulum
ETC	Electron Transport Chain
FAD	Familial Alzheimer's disease
HATU	2-(1H-7-Azabenzotriazol-1-yl)--1,1,3,3-tetramethyl-uronium hexafluorophosphate Methanaminium
i.c.	Intracerebral
IMR-32	Human neuroblastoma cell line
IL-1 β	Interleukin – 1 Beta
i.p.	Intraperitoneal
Leu	Leucine
MALDI TOFMS	Matrix Assisted Laser Desorption Ionisation Time of Flight Mass Spectrometry

MEPTIDES	Poly <i>N</i> -methylated Amyloid- β - peptide (A β) C-terminal fragments
Met	Methionine
NFTs	Neurofibrillary Tangles
NPH	Normal-pressure hydrocephalus
PS	Phosphatidyl Serine
PS1	Presenelin 1 gene
PS2	Presenelin 2 gene
PT	Permeability Transition
qPCR	Quantitative real time Polymerase chain reaction
ROS	Reactive oxygen species
SAD	Sporadic Alzheimer's disease
SEM	Standard error of the mean
SD	Sprague-Dawley
TACE	TNF- α converting enzyme
TNF- α	Tumor necrosis factor alpha
TRAIL	TNF- α related apoptosis-inducing ligand
4HNE	4 - Hydroxynonenal

TABLE OF CONTENTS

PAGE

Declaration	i
Acknowledgements	ii
Presentations	iii
List of abbreviations	iv
Table of contents	vi
Index: List of figures	x
Abstract	xiv

TABLE OF CONTENTS		PAGE
CHAPTER 1	INTRODUCTION	1
1.0	Preamble	1
1.1	Introduction	1
1.2	Classification of Alzheimer's disease (AD)	2
1.3	Aetiology of AD	2
1.4	Neurofibrillary tangles (NFT)s	3
1.5	Models of AD	3
1.6	Amyloid- β ($A\beta$) homeostasis	4
1.6.1	Amyloid Precursor Protein (APP)	4
1.6.2	Secretase enzymes	5
1.6.3	$A\beta$ pathology	7
1.7	Inflammation	7
1.8	Oxidative stress	9
1.9	Apoptosis	11
1.10	Manifestations of AD	14
1.11	Diagnosis	15
1.12	Conventional management therapies	16
1.13	Poly - <i>N</i> - methylated Amyloid - β - Peptide ($A\beta$) <i>C</i> - terminal Fragments (MEPTIDES)	18
1.14	Basis of the study	19

1.14.1	Aims	19
--------	------	----

CHAPTER 2	MATERIALS AND METHODS	20
------------------	------------------------------	-----------

2.1	Materials and Methods	20
-----	-----------------------	----

2.1.1	Reagents and Materials	20
-------	------------------------	----

2.1.2	Ethical clearance	21
-------	-------------------	----

2.1.3	Animals	21
-------	---------	----

2.2	Experimental design and timeline	22
-----	----------------------------------	----

2.3	Stereotaxic surgery	24
-----	---------------------	----

2.4	Learning and Memory tests	25
-----	---------------------------	----

	The Morris water maze	
--	-----------------------	--

2.5	Sacrifice	26
-----	-----------	----

2.6	Biochemical Assays	26
-----	--------------------	----

2.6.1	Real Time PCR	26
-------	---------------	----

2.6.2	Enzyme-linked immunosorbent assay (ELISA)	27
-------	--	----

2.6.3	Western blotting	28
-------	------------------	----

2.6.4	Matrix Assisted Laser Desorption Ionization Time of Flight Mass Spectrometry(MALDI-TOF MS)	29
-------	--	----

2.6.4.1	MALDI IMS matrix conditions	29
---------	-----------------------------	----

2.6.4.2	MALDI IMS detection limits and MS/MS verification	30
2.6	Data presentation	31
	CHAPTER 3	RESULTS
	Study A	32
3.1	Behavioural results	32
3.2	TNF- α results	33
3.3	4HNE Western blot results	33
	Study B	
3.4	Behavioural results	38
3.5	C3 qPCR results	38
3.6	C3 Western blot results	39
3.7	MALDI TOF MS results	39
	CHAPTER 4	DISCUSSION
	CHAPTER 5	SUMMARY AND CONCLUSION
5.0	Summary	53
5.1	Conclusion	53

Index

List of Figures

CHAPTER 1

Figure 1.1: Diagram showing APP cleavage by secretase enzymes in the amyloidogenic/non - amyloidogenic pathways. 6

Figure 1.2: Diagram showing how several conditions including A β aggregation may lead to increased oxy-radicals resulting in membrane lipid peroxidation and generation of lipid peroxidation adducts like 4HNE that may alter membrane ATPases which leads to increased intracellular Ca²⁺ levels that may cause a further increase in ROS and ultimately cause cell death. 11

Figure 1.3: Diagram showing intracellular sources of ROS and their interaction with apoptotic pathways. 12

Figure 1.4: Diagram showing nitric oxide (NO) neurotoxicity and neuroprotectivity in relation to AD. 13

Figure 1.5: Research directions and strategies in the search for disease-modifying DRUGS. 18

Figure 1.6: Diagram showing Molecular structure of MEPTIDES. 19

CHAPTER 2

Figure 2.1: Diagram showing experimental design and timeline for study A and B. 22

Figure 2.2: Diagram showing Morris Water Maze tank. 25

CHAPTER 3

Figure 3.1: Graph showing time taken by TB-injected and A β_{42} -injected rats to find the hidden platform in the MWM. The pre-injection test is the test before the i.c injection of TB or A β_{42} (10 μ l, i.c., bilaterally) to create lesions similar to those observed in AD. The significant difference observed between the A β_{42} pre-injection test vs A β_{42} post-injection test (18.20 ± 7.28 vs 49.60 ± 10.22 , * $p < 0.05$), shows a decrease in ability to recall the location of the platform in the rats injected with A β_{42} . The significant difference observed when A β_{42} post-injection test was compared to TB pre and post-injection tests (49.60 ± 10.22 vs 23.30 ± 8.07 and 49.60 ± 10.22 vs 16.10 ± 4.22 , * $p < 0.05$), show that TB- i.c. injections did not impair recall ability of the control rats in the MWM.

34

Figure 3.2: Diagram showing percentage change in the time taken to find the hidden platform in the MWM when the post- i.c. injection test of the TB- and A β_{42} -injected rats was compared to the pre- i.c. injection test of the same rats in their respective groups. The pre - injection test was taken as 100 % for all comparisons. Figure 3.2 A shows post- vs pre- i.c. injection test of the TB-injected rats. Sixty percent of the rats in this group showed decreased time to reach the hidden platform vs the 40 % that showed an increased time to reach the hidden platform. Figure 3.2 B shows post- vs pre- i.c. injection test of the A β_{42} -injected rats. Eighty percent of the rats in this group showed an increased time to reach the hidden platform vs 20% that showed a decreased time to reach the hidden platform.

35

Figure 3.3: Graph showing expression of TNF- α in the dorsal hippocampus of TB vs A β_{42} -injected rats. The t-test analysis of our TNF- α results did not show any significant difference (519 ± 186.70 vs 5032 ± 440.40 , $p > 0.05$) when the TB and A β_{42} -injected groups were compared.

36

Figure 3.4: Graph showing 4HNE Western blot results obtained for the dorsal hippocampi of A β ₄₂- vs TB-injected. The t-test analysis showed that there was no significant difference between the 2 groups (4.600 ± 0.35 vs 4.30 ± 0.61 , $p > 0.05$).

37

Figure 3.5: Graph showing time taken by MEPTIDES-treated TB-injected and A β ₄₂-injected rats to find the hidden platform in the MWM. The significant difference observed between the pre-injection test vs the post-injection test 1, which is the first test before i.p. injection of MEPTIDES in the A β ₄₂-injected group (17.60 ± 4.24 vs 56.00 ± 12.41 , $*p < 0.05$) shows a decrease in ability to recall the location of the platform in the rats injected with A β ₄₂ and is similar to that of the A β ₄₂-injected group in Figure 3.1. This time however, was significantly reduced 24 hours after the first i.p. injection of MEPTIDES in the same A β ₄₂-injected group (56.00 ± 12.41 vs 21.50 ± 5.27 , $^{\#}p < 0.05$).

40

Figure 3.6: Graph showing qPCR expression of the C3 gene in the dorsal hippocampal tissue of TB- and A β ₄₂-injected rats vs MEPTIDES (2 mg/kg)-treated TB- and A β ₄₂-injected rats. The i.c A β ₄₂ injection significantly increased the expression of the C3 gene when the A β ₄₂-injected rats were compared to TB-injected rats (2.54 ± 0.45 vs 1.16 ± 0.11 , $*p < 0.05$). Three injections of MEPTIDES (2 mg/kg, i.p.) over a 3-day period reversed the effect of A β ₄₂ on C3 gene expression when A β ₄₂-injected rats were compared to the MEPTIDES-treated A β ₄₂ rats (2.54 ± 0.45 vs 0.77 ± 0.04 , $*p < 0.05$).

41

Figure 3.7: Graphs showing Western blot results for C3 protein levels in dorsal hippocampal tissue of TB-injected, A β -injected, and MEPTIDE (2 mg/kg)-treated rats. The t-test analysis of TB- vs A β -injected rats did not show any significant difference in dorsal hippocampal C3 levels (1.38 ± 0.09 vs 1.55 ± 0.27 , $p > 0.05$), (Figure 3.7 A). The t-test analysis of the MEPTIDE (2 mg/kg)-treated TB- vs A β -injected rats also did not show any significant difference when the 2 groups were compared (0.19 ± 0.04 vs 0.11 ± 0.01 , $p > 0.05$), (Figure 3.7 B).

42

Figure 3.8: Diagrams showing presence and abundance of MEPTIDES derived metabolites in the rat brain. Figure 3.8 A shows naïve brain. Figure 3.8 B shows TB-injected MEPTIDES-treated rat brain. Figure 3.8 C shows A β ₄₂-injected MEPTIDES-treated rat brain. There was a higher abundance of the Na⁺/K⁺ adduct of the (690.04 ± 0.20 % and 674.13 ± 0.20 % m/z respectively) fragments in the MEPTIDES-treated A β ₄₂-injected brain (Figure 3.8 C) when it was compared to the MEPTIDES-treated TB-injected brain (712.41 ± 0.20 % m/z) (Figure 3.8 B). This peak was not observed in the control naïve brain (Figure 3.8 A). The peak of interest (712.41 ± 0.20 % m/z) in all MALDI TOF MS results is indicated by the red line. The colour legend represents the intensity of the peak of interest.

ABSTRACT

Introduction

Alzheimer's disease (AD), a progressive neurodegenerative disorder that affects mostly the limbic system and the neocortical areas of the brain, is the most prevalent form of dementia affecting the elderly population. Twenty-nine million people live with the disease worldwide, 10% of the population > 65 years of age and 50 % of the population > 85 years of age. These figures are expected to increase exponentially over the next few decades and reach 81.1 million by the year 2040. Hallmark lesions include extracellular deposition of β -amyloid protein ($A\beta$) fibrillar plaques and intraneuronal neurofibrillary tangles (NFTs), which impair synaptic plasticity in the target regions of the brain thereby producing a progressive decline in cognitive function, with the earliest signs observed in learning and memory. Current therapies of AD are merely palliative and only slow down cognitive decline. In a recent study a novel compound, poly-*N*-methylated amyloid beta ($A\beta$)-peptide C-terminal fragments (MEPTIDES) was shown to reduce $A\beta$ toxicity *in vitro* and in *Drosophila melanogaster*, however whether this novel drug is equally effective in mammals to inhibit $A\beta$ -induced toxicity remains unclear. Accordingly in the present study we investigated the effects of MEPTIDES on the neurotoxicity induced by a single intracerebral (i.c.) injection of $A\beta_{42}$ into the dorsal hippocampus of adult male Sprague-Dawley (SD) rats, a model of AD-like impaired learning and memory, and explored the implications of these findings for possible future management therapies or AD.

Methods

Ethical clearance (ref: 048/13/Animal) was obtained from the University of KwaZulu-Natal Ethics Committee. Fully grown male SD rats (n = 40, 300 - 350 g, 8 - 9 weeks of age at the beginning of the study) were used. The study was divided into 2 parts. In part A, a rat model (n = 20) of impaired learning and memory was established using $A\beta_{42}$ (2 mM). A total of 100 μ g of the neurotoxin was injected bilaterally into the dorsal hippocampus at a rate of 1 μ l/ minute. In part B, the effect of MEPTIDES (2 mg/kg) injected intraperitoneally (i.p.) on $A\beta_{42}$ -induced neurotoxicity was investigated *in vivo* (n = 20). Control rats received intra-hippocampal injections of vehicle (Tris buffer, TB, 0.15 M). Learning and memory tests were performed using the Morris water maze. MEPTIDES were administered i.p. for 3 days post the i.c. injection of

A β ₄₂. Caspase 3 (C3), Tumor Necrosis factor Alpha (TNF- α), and 4-Hydroxynonol (4HNE) levels were measured in hippocampal tissue by either qPCR, Western Blot, or ELISA. MALDI TOF MS was used to determine whether MEPTIDES cross the blood brain barrier (BBB) and their distribution in the rat brain thereof.

Results

Behavioural results showed spatial learning and memory deficits in rats that were injected with A β ₄₂. These animals also displayed upregulation of C3 in the dorsal hippocampus. These effects were reversed in the rats that received i.p. injections of MEPTIDES, 24 hours after intra-hippocampal injection of A β ₄₂. C3 cascade disruptions appeared to be amongst the earliest markers of A β ₄₂-induced neurotoxicity.

Discussion and Conclusion

Findings from this study showed that a single i.c. injection of A β ₄₂ induces C3 cascade and behavioural deficits in an adult male SD rat. i.p. injections of MEPTIDES, 24 hours after intra-hippocampal injection of A β ₄₂ reversed these effects.

Keywords: Alzheimer's disease, MEPTIDES, A β ₄₂, Morris water maze, caspase 3

CHAPTER 1

Literature Review

1.0 Preamble

Alzheimer's disease (AD) is a poly-aetiological neurological disorder that leads to dementia (Sipos et al., 2007). The disease hallmarks include extracellular deposition of amyloid- β protein (A β) and intraneuronal neurofibrillary tangles (NFTs). The earliest symptoms include learning and memory deficits (U.S. Alzheimer's Association, 2011). A novel compound, MEPTIDES, which is synthesized from C-terminal fragments of A β (covering residues 31 - 42 or parts thereof), has been shown to reduce toxicity of A β *in vitro* and in *Drosophila melanogaster* (Pratim Bose et al., 2009), but its effects on A β neurotoxicity *in vivo* still remain elusive. Accordingly, this study investigated the effects of MEPTIDES *in vivo* on A β ₄₂-induced neurotoxicity in an adult male Sprague-Dawley (SD) rat model of learning and memory, which may have implications for AD management and treatment therapies.

1.1 Introduction

AD is a progressive neurodegenerative disorder that affects mostly the limbic system and the neocortical areas of the brain (Sipos et al., 2007). AD presents clinically as an inexorable cognitive impairment and a significant decline in performance of activities of daily living as it progresses. AD is the most prevalent form of dementia affecting the elderly population (U.S. Alzheimer's Association, 2011). Females are more prone to suffer from AD than males due to differences in hormonal profiling (Mathew et al., 2011), even after correcting for differences in life expectancies (Kumar et al., 2011). AD is associated with a number of risk factors which include aging, family history, apolipoprotein E4 (ApoE4), hypercholesterolaemia (Huang et al., 2007), diabetes, hypertension, high alcohol intake and vascular diseases (Findeis, 2007). Data show that 29 million people live with the disease worldwide (Reddy, 2011), 5.4 million in the U.S. alone (U.S. Alzheimer's Association, 2011), and these figures are expected to increase exponentially over the following decades (U.S. Alzheimer's Association 2011; Cole and Vassar, 2007) and reach 81.1 million by the year 2040 (Chu, 2012).

1.2 Classification of Alzheimer's disease

There are basically 2 forms of AD. One is early onset Familial Alzheimer's disease (FAD) which is caused by autosomal dominant mutations in either Amyloid Precursor Protein (APP) or Presenilin 1 or 2 (PS1/PS2) genes (Mathew et al., 2011). FAD accounts for approximately 2% of all AD cases. Mutations in these genes may cause an increase or decrease in the production of $A\beta_{42}$ (Findeis, 2007), an increase in the production may lead to 100% penetrance of the disease (Cole and Vassar, 2007). Presenilin 1 gene mutations are the most common among FAD mutations (Chu, 2012). The second form is late onset Sporadic Alzheimer's disease (SAD) which accounts for approximately 98% of all AD cases and the underlying causes of this AD type remain elusive (Mathew et al., 2011).

It is estimated that the costs for dementia care worldwide are in the region of 315.4 billion U.S. Dollars annually (U.S. Alzheimer's Association, 2007). In 2012, the total worldwide societal cost of dementia was estimated to be US\$ 422 billion (Chu, 2012). Blocking disease progression or, in the best case scenario, preventing AD altogether would not only have significant benefits to the patient and their families, but would also substantially lighten the enormous economic burden to the community at large. Since the majority of AD cases arise from sporadic causes, the bulk of scientific investigations have thus focused on this dementia type.

1.3 Aetiology of AD

AD has 2 hallmark lesions namely, extracellular deposition of $A\beta$ protein fibrillar plaques and intraneuronal NFTs (Mamelak, 2007), but it still remains unclear whether these are the cause of AD (Heneka and O'Banion, 2007). Evidence suggests that altered metabolism is a very early change in AD and that oxidative stress, particularly in lipids, proteins and DNA (Irie et al., 2005) of vulnerable neurons (Mamelak, 2007), precedes plaque formation (Gibson, 2002). $A\beta$ has been shown to disrupt calcium (Ca^{2+}) homeostasis by increasing the density of L and N-type voltage-dependent Ca^{2+} channels (Freir et al., 2003) and enhancing the influx of Ca^{2+} into hippocampal neurons through these channels. This suggests that Ca^{2+} channels may play a role in the pathogenesis of AD (Freir et al., 2003). Additional neuropathologies include reactive microglial cells, increased expression of apoptotic protein

features, dystrophic neurons and bundles of astrocytic processes (Mamelak, 2007) as well as cholinergic, dopaminergic and serotonergic dysfunctions (Mandel et al., 2007).

1.4 Neurofibrillary tangles (NFTs)

NFTs consist of paired helical filaments that are composed of abnormally hyperphosphorylated microtubule-associated tau protein (Fen et al., 2010). Tau is predominantly expressed in neuronal axons (Reddy, 2011), and has more than 30 phosphorylation sites. Tau phosphorylation regulates microtubule assembly and plays a role in the outgrowth of neuronal processes, regulation of the intricate transport system of the neuron, and the development of neuronal polarity (Reddy, 2011). In contrast, hyperphosphorylated tau becomes pathological destabilizing microtubules, resulting in the aggregation of hyperphosphorylated tau (Reddy, 2011). Increased evidence suggests that tau is critically involved in AD pathogenesis, particularly in impairing axonal transport of APP and subcellular organelles including mitochondria in neurons affected by AD (Reddy, 2011). Recent data reviewed by Reddy (2011) demonstrated that A β production, accumulation and A β -induced oxidative stress are critical factors for the hyperphosphorylation of tau in AD neurons, which ultimately leads to the production of NFTs. Neurons with NFTs show extensive oxidative stress, suggesting that oxidative stress plays a vital role in the pathophysiology of AD (Gibson, 2002). NFTs are arguably the most important aspect of the degenerating phenotype in AD-affected neurons (Perry et al., 2002).

1.5 Models of AD

Genetics play an important role in the manifestation of AD and AD-associated genes, which may be divided into those in which mutations cause autosomal dominant AD and those which polymorphisms serve as risk factors for AD, have paved the way for the development of AD mouse models (Hall and Roberson, 2012). The oldest and most commonly used transgenic models based on the expression of human APP (hAPP) have contributed enormously to the testing of the Amyloid hypothesis, several therapeutic agents and more recently, biomarkers that can assist in the detection of asymptomatic AD (Hall and Roberson, 2012).

Traditionally, mice have been chosen over rats for transgenesis owing to technical reasons, but rats offer more advantages than mice because their lineage is closer to that of humans in several physiological and functional aspects (Hall and Roberson, 2012). The range of

advantages that rats offer include, larger body surface area and brain size which facilitate intracerebral administration of different experimental compounds as well as neurosurgical and neuroimaging experiments. The major advantage that rats offer is behavioural characterization because of their finer motor coordination when compared to that of mice (Hall and Roberson, 2012). A complete model of AD would have to display the full spectra of the underlying clinical and pathological symptoms of AD, no presently existing model exhibits all the features of AD, existing models develop phenotypes of AD to different extents and combinations (Hall and Roberson, 2012). The model of bilateral i.c. injections of A β ₄₂ into the dorsal hippocampus of a rat brain that we used in the present study was adopted from a study done by Shin et al. (1997), and was modified to answer specifically, the questions that were asked by our study.

1.6 A β homeostasis

APP processing is found to be somewhat heterogeneous, resulting in the production of variable lengths of A β , particularly at the carboxyl terminus (Cole and Vassar, 2007). The two major forms of A β that have been observed to be produced in the processing of APP are, 40 and 42 residues in length, A β ₄₀ (produced as a cellular antioxidant) and A β ₄₂ (has been shown to be neurotoxic), respectively (Findeis, 2007). In a normal individual, the majority of the A β produced is of the shorter variety, A β ₄₀ (Cole and Vassar, 2007). Cerebral A β levels are regulated by the production, clearance and degradation of A β (Reddy, 2011). APP metabolism may also play a role in tau phosphorylation and subsequent NFT formation (Cetin, 2013).

1.6.1 Amyloid Precursor Protein (APP)

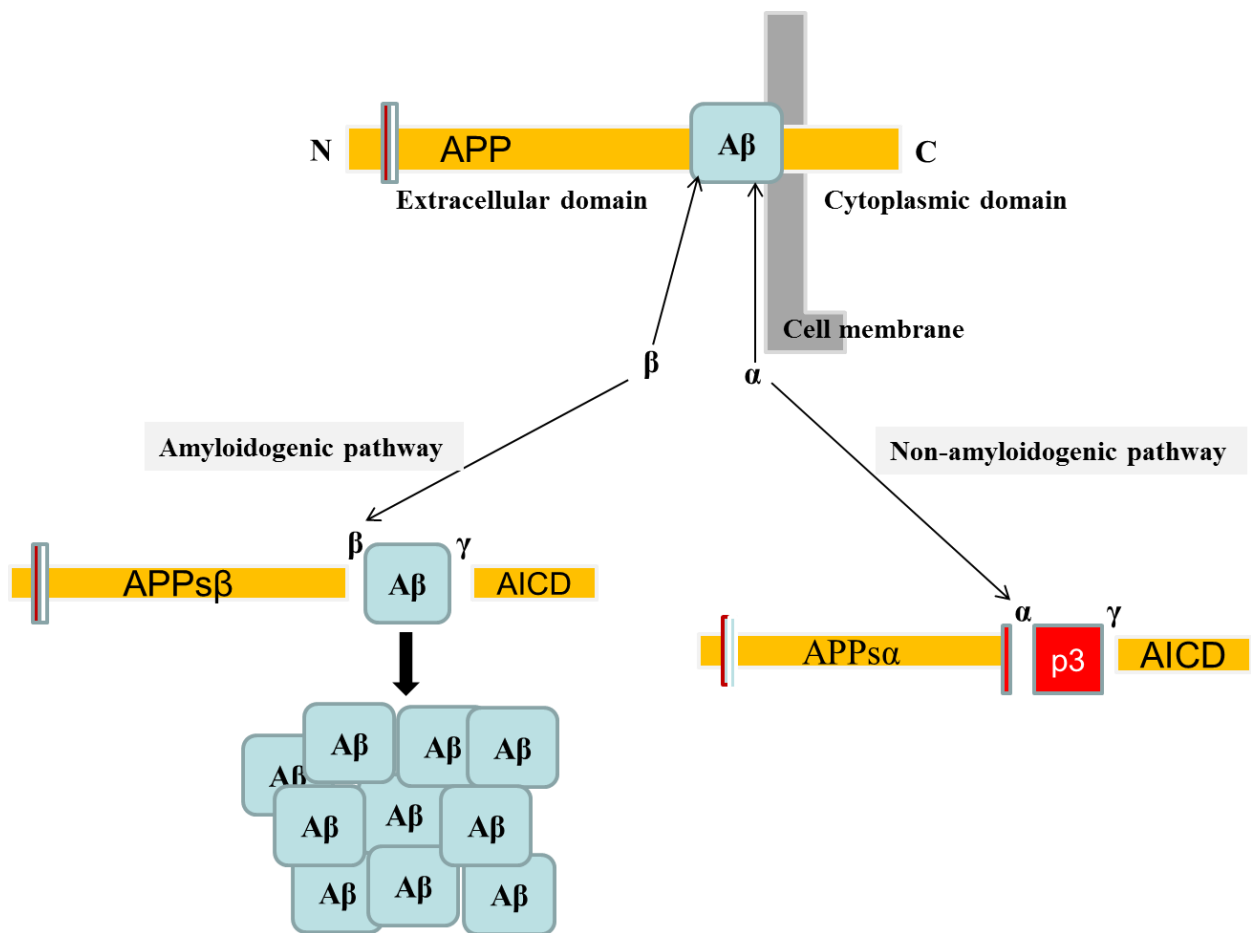
APP is a type-I transmembrane protein that has 695-770 amino acids (AAs) (Mathew et al., 2011). It is transported from endoplasmic reticulum (ER) to the cell surface via a secretory pathway and has a large extracellular hydrophilic *N*-terminus, and a small cytoplasmic *C*-terminus (Mathew et al., 2011). The APP gene is located on chromosome 21 and mutations in this gene may either increase or decrease A β production (Findeis, 2007).

1.6.2 Secretase enzymes

β -Secretase is a novel aspartyl protease known as β -site APP-cleaving enzyme (BACE1) (Cole and Vassar, 2007), a type-I membrane protease with 501 AAs from the pepsin-like class of protease enzymes (Barman and Prabhakar, 2013). It is the rate-limiting enzyme in the synthesis of A β and therefore the prime drug target for lowering cerebral A β levels in the management, treatment and prevention of AD (Cole and Vassar, 2007). γ -Secretase is a complex of proteins consisting of presenilin 1 or 2 (PS1/PS2), nicastrin, anterior pharynx-defective 1 (Aph1) and presenilin enhancer 2 (Pen2). α -Secretase is TNF- α converting enzyme (TACE), a member of the disintegrin and metalloprotease domain protein (ADAM) family (Cole and Vassar, 2007).

BACE1 utilizes the general acid base mechanism to cleave the peptide bond during its catalytic cycle (Barman and Prabhakar, 2013). It initiates synthesis in the amyloidogenic pathway at the Asp+1 residue of APP to form the *N*-terminus of A β . The scission results in two cleavage fragments, a secreted APP ectodomain (APPs β) and a membrane bound carboxyl terminal fragment (CTF) that is subsequently cleaved by γ -secretase to generate the *C*-terminus of A β and an APP intracellular domain (AICD) which is released into the cytosol (Cole and Vassar, 2007), and thus migrates to the nucleus (Mathew et al., 2011) where it plays a role in transcriptional transactivation (Cole and Vassar, 2007) by regulating phosphoinositide-mediated Ca²⁺ signaling through a γ -secretase-dependent signaling pathway (Findeis, 2007).

In the alternate non-amyloidogenic pathway, α -secretase cleavage occurs within the A β domain at Leu+17 residue of APP. The scission produces a secreted (APPs α) ectodomain and a CTF which in turn is cleaved by γ -secretase to form a 3kDa fragment p3 (Cole and Vassar, 2007). APPs α activates a putative receptor on the neuronal membrane which initiates a series of reactions that lead to the opening of potassium (K⁺) channels (Mathew et al., 2011). This ultimately leads to the activation of nuclear transcription factor kappa β (NFk β), which promotes cell survival (Mathew et al., 2011).



Key: N/C – N/C-terminus of APP, APP – Amyloid precursor protein, A β – Amyloid beta, $\beta/\alpha/\gamma$ – Beta/Alpha/Gamma secretase enzymes, AICD – APP intracellular domain

Figure 1.1: Diagram showing APP cleavage by secretase enzymes in the amyloidogenic/non - amyloidogenic pathways. Image adapted from Cole and Vassar (2007).

Although the majority of body tissues exhibit β -secretase activity, the highest levels are observed in neuronal cell lines and brain tissue with optimal activity detected at an acidic pH of 4.5 within subcellular compartments of the secretory pathway (the trans-Golgi network and endosomes) (Cole and Vassar, 2007).

1.6.3 A β Pathology

A β_{42} is a 4kDa (Mathew et al., 2011) amphiphilic protein (Bose et al., 2009), that accounts for about 5-15 % of the total A β pool in a normal individual (Findeis, 2007). It is generated following abnormal sequential cleavage of the transmembrane APP by β - and γ -secretase in the amyloidogenic pathway (Fen et al., 2010), (see figure 1.1). The A β_{42} protein subsequently aggregates and forms higher order oligomers that directly interact with the cell membrane through the receptor for advanced glycation end products (AGEs) (Behl and Moosmann, 2002) but the molecular mechanisms underlying the generation of soluble oligomers, insoluble fibrils, other neurotoxic species and their aggregation (Crews et al., 2010) are not fully understood (Bose et al., 2009). Synthesis of A β_{42} is precluded if APP is cleaved by α -secretase within the A β domain in the non-amyloidogenic pathway. β - and α -Secretase moieties compete for APP substrate and hence an increase in the amyloidogenic pathway is coupled with a reciprocal decrease in the non-amyloidogenic pathway and vice versa (Cole and Vassar, 2007).

In this study we particularly focused on oxidative stress, apoptosis, and inflammation mediated by stereotaxic infusion of A β_{42} into the dorsal hippocampus of an adult male SD rat model of learning and memory. We also investigated the effectiveness of MEPTIDES *in vivo* in the prevention and/or reduction of A β -induced neurotoxicity which may support MEPTIDES as a possible anti-AD drug which is beneficial in preventing or slowing down cognitive decline.

1.7 Inflammation

While minor signs of neuroinflammation can be found in a normal aging brain, the AD brain displays increased activation of inflammatory systems suggesting that qualitatively different immunostimulants may exist in the latter (Heneka and O'Banion, 2007). Although synthesis and deposition of A β and NFTs are hallmarks of AD (Mamelak, 2007, Heneka and O'Banion, 2007), evidence suggests that inflammation in pathologically vulnerable regions of the AD brain (Akiyama et al., 2000) represents the third hallmark (Heneka and O'Banion, 2007). Damaged neurons and neurites and highly insoluble A β peptide deposits and NFTs provide stimuli for inflammation in the AD brain (Akiyama et al., 2000). Microglia represent the innate immune system in the brain and express a wide array of receptors that detect foreign

particles and tissue damage (Cameron and Landreth, 2010). Toll-like receptors (TLRs) are the most prominently expressed receptors in microglia, with TLR 2, 4 and TLR co-receptor, CD14, being of importance in AD (Cameron and Landreth, 2010). Following activation, various neuro-inflammatory (pro and anti-inflammatory) mediators, including a wide array of neurotoxic cytokines and chemokines are produced and released by microglia, which may also result in recruitment of astrocytes and neurons to the inflammatory response, and this cascade is thought to actively enhance the inflammatory response to extracellular A β plaques (Heneka and O'Banion, 2007). Astrocytes are involved in the degradation and clearance of A β , and provide trophic protection of neurons by forming a protective barrier between neurons and A β plaques (Heneka and O'Banion, 2007). Increased astrocyte number associated with A β lesions in AD suggests that these aggregates produce chemotactic molecules that recruit astrocytes (Heneka and O'Banion, 2007). Once this inflammation is initiated by degeneration, it may significantly contribute to disease progression and chronicity (Heneka and O'Banion, 2007).

While inflammation is thought to be secondary to degeneration, evidence suggests that microglia and astrocytes (Heneka and O'Banion, 2007) may be activated by endogenous proteins which increase the production of inflammatory cytokines (Heneka and O'Banion, 2007) like Interleukin-1 β (IL-1 β), Tumor necrosis factor alpha (TNF α) (Rogers et al., 1996) which regulate the intensity and duration of the inflammatory response (Heneka and O'Banion, 2007). In AD these have been observed to enhance APP processing by upregulating β -Secretase, altering A β fibrillar protein production and/or metabolism (Rogers et al., 1996) therefore increasing neurotoxic secretory products, pro-inflammatory cytokines and ROS (Eikelenboom and van Gool, 2004) which establishes a vicious cycle (Heneka and O'Banion, 2007) that greatly contributes to neuronal damage. TNF- α , a pro-inflammatory cytokine and a focus in the present study, exhibits both pro-apoptotic and anti-apoptotic properties that account for the majority of the neurotoxic effects of proteins secreted by microglia in the CNS (Heneka and O'Banion, 2007). Nearly all cytokines that have been studied in animal models of AD, primarily in immunohistological evaluations, including IL-1 β , IL-6 and TNF α were upregulated when compared to their control equivalents (Akiyama et al., 2000). These differences are less likely to be a result of genetic polymorphisms that have been previously described (Nicoll et al., 2000, Papassotiropoulos et al., 1999, McCusker et al., 2001) because none of the members of the cytokine family that are associated with AD map onto the chromosomal region with evidence of a genetic linkage (Tanzi and Bertram,

2005) that increases the risk of AD development later in life. In an article by Akiyama et al. (2000), TNF α was reported to be neuroprotective in the AD brain. It is this controversy that inspired our research team to investigate whether TNF α is up or downregulated in our animal model of A β -induced memory impairment and to subsequently establish what the implications of these changes are.

1.8 Oxidative stress

Reactive oxygen species (ROS) play an important role in the regulation of normal cellular and thus body function when they are produced at low concentrations at the appropriate time and place but when they are produced in excess, they can have detrimental consequences particularly for mitochondrial function and ultimately cellular integrity, a state known as oxidative stress (Rosenfeldt et al., 2013). ROS may target any cell component, but they generally react with the first structure they encounter, which is frequently the lipid bilayer of cell membranes. Oxidative stress represents an imbalance in the production of ROS and the body's antioxidant defense system's ability to detoxify the reactive intermediates (Rosenfeldt et al., 2013). The body has developed natural defense systems such as endogenous antioxidants that counteract the destructive effects of ROS and maintain REDOX equilibrium thus ensuring optimal health (Perry et al., 2002). Various intrinsic enzymatic and non-enzymatic pathways are involved in achieving this REDOX equilibrium (Perry et al., 2002). The cytopathological significance of oxidative damage is seen by the upregulation of antioxidant enzymes (Mamelak, 2007). Sources of ROS include enzymatic activation of cytochrome C, NADPH oxidases, xanthine oxidase, dysregulation of endothelial nitric oxide synthase (eNOS) and leakage from mitochondria. The brain is a logical target for free radical damage due to its high concentration of unsaturated lipids, catecholamines and increased rate of oxidative metabolism (Mamelak, 2007, Lee et al., 2012). The brain also has low concentrations of enzymatic antioxidants and non-enzymatic free radical scavengers, whilst certain areas contain large amounts of iron (Fe) which is a crucial cofactor in ROS generation (Mamelak, 2007). This suggests that oxidative stress contributes to brain aging, but is by no means the sole cause of brain senescence (Mamelak, 2007).

Oxidative insults that induce neuronal apoptosis, including agents that induce membrane lipid peroxidation, have been shown to activate caspases (Cetin, 2013). Damage caused by oxidative radicals observed in AD includes AGEs, nitration, lipid peroxidation adduction

products as well as carbonyl-modified neurofilament protein and free carbonyls (Mamelak, 2007). This damage involves all neurons vulnerable to death in AD and not only those containing NFTs (Mamelak, 2007). Lipid peroxidation disrupts the $\text{Na}^+/\text{Ca}^{2+}$ channels and glucose uptake which leads to apoptosis (Mathew et al., 2011). The free radical theory of ageing proposes that, prolonged pro-oxidant status generated during normal cellular metabolism causes cumulative damage to DNA and other macromolecules (Mamelak, 2007). It also suggests that free radicals and their reactions are involved in the aetiology and development of a number of life-limiting diseases (Mamelak, 2007). Increased mitochondrial DNA in the early stages of AD may be linked to increased oxidative potential (Mamelak, 2007). Haem oxygenase (HO-1) is among the most sensitive indicators of the cellular oxidative stress response and it has been shown that both HO-1 and its mRNA are increased in the brains of patients with AD (Mamelak, 2007). In a review by (Mamelak, 2007) it is suggested that increased HO-1 expression co-localizes with the altered form of tau protein. The most crucial aspect of oxidative damage in AD pathogenesis appear to be the cytoskeletal modifications (e.g. NFTs, are the most obvious modification and are the important phenotype in a degenerating neuron) in neurons that are susceptible to damage in AD, which in turn plays a key role in the irreversible cellular dysfunctions that ultimately yield dementia (Mamelak, 2007).

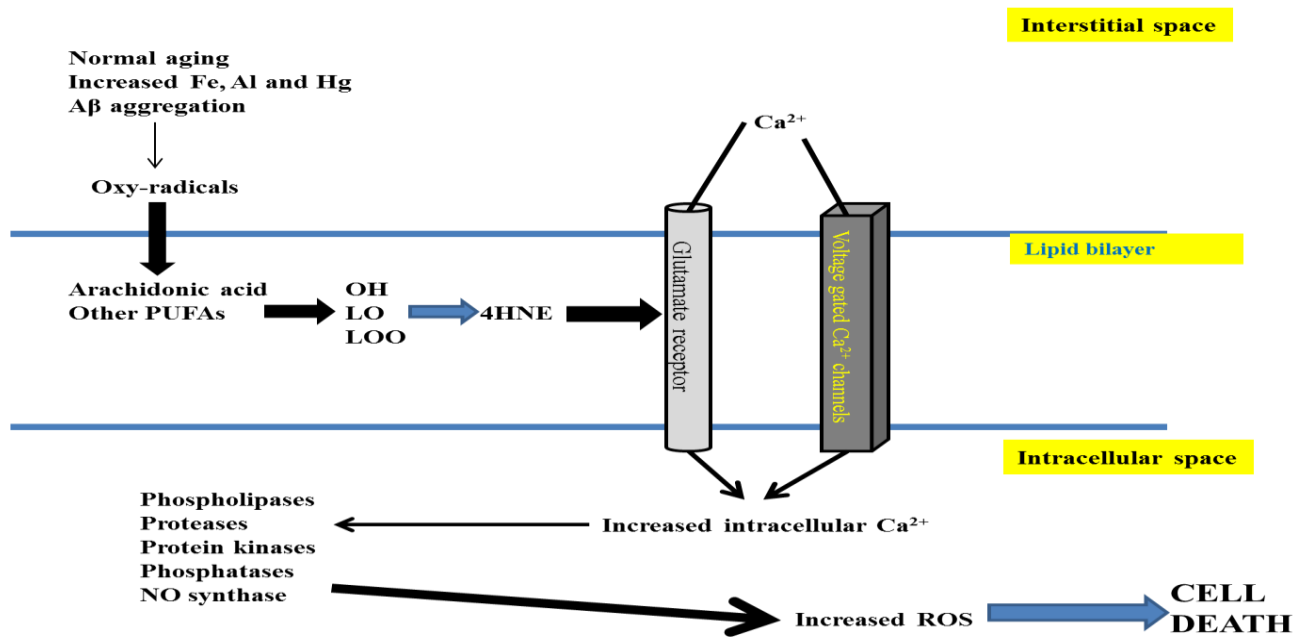


Figure 1.2: Diagram showing how several conditions including A β aggregation may lead to increased oxy-radicals resulting in membrane lipid peroxidation and generation of lipid peroxidation adducts like 4HNE that increase intracellular Ca²⁺ levels that may cause a further increase in ROS and ultimately cause cell death. Image adapted from Cetin (2013).

1.9 Apoptosis

Apoptosis is a highly regulated process involved in embryonic development, developmental tissue remodeling, normal cell turnover and is a cell death program central to cellular and tissue homeostasis (Cetin, 2013). Apoptosis is increased in the aging process due to increased oxidative stress (Cetin, 2013) and is characterized morphologically by a series of events that include cytoplasmic shrinkage, chromatin condensation, nuclear and cellular fragmentation, and the formation of apoptotic bodies. Dysregulation in apoptotic pathways results in excessive or insufficient cell death that may result in several pathological processes leading to disease states such as cancers, autoimmune syndromes and/or neurodegenerative diseases like AD.

Caspases are a family of intracellular cysteine-aspartate proteases that are divided into initiators of apoptosis (caspases-2, -8, -9 and -10), and effectors of apoptosis (caspases-3, -6, -7 and -14), however some caspases, including caspase-3 (C3) and caspase-6 (Casp6), appear

to function as both initiators and effectors (Cetin, 2013). Caspases are not only essential for triggering apoptosis, they have also been shown to play key roles in other non-apoptotic pathways, such as differentiation and proliferation of diverse cell types, axon guidance and synaptic activity and plasticity (Cetin, 2013). Activation of caspases has been implicated in several neurodegenerative diseases, such as AD, Huntington’s disease (HD), various ataxias and amyotrophic lateral sclerosis (Cetin, 2013).

Cells undergo apoptosis through two major pathways, the extrinsic pathway (death receptor pathway) (Zeng et al., 2012) and the intrinsic pathway (the mitochondrial pathway) (Romani et al., 2010). These two pathways can be linked by caspase-8-activated truncated Bid formation. Very recently, death receptor 6 (DR6) also known as TNFRSF21, a relatively new member of the death receptor family was shown to be involved in the neurodegeneration observed in AD (Zeng et al., 2012). It was found that DR6 induces apoptosis when it is overexpressed (Zeng et al., 2012). However, how the death signal mediated by DR6 is transduced intracellularly is not known. Although caspases are the main players involved in apoptosis, there are other molecules involved in the progression of the apoptotic cascade that are relevant to AD (Cetin, 2013).

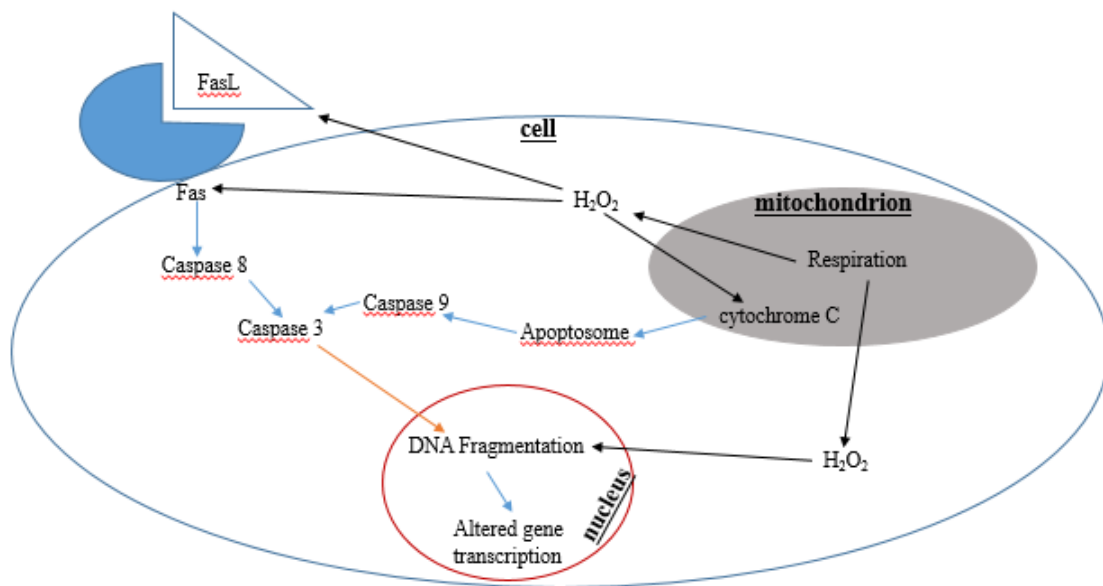


Figure 1.3: Diagram showing intracellular sources of ROS and their interaction with apoptotic pathways (Cetin, 2013)

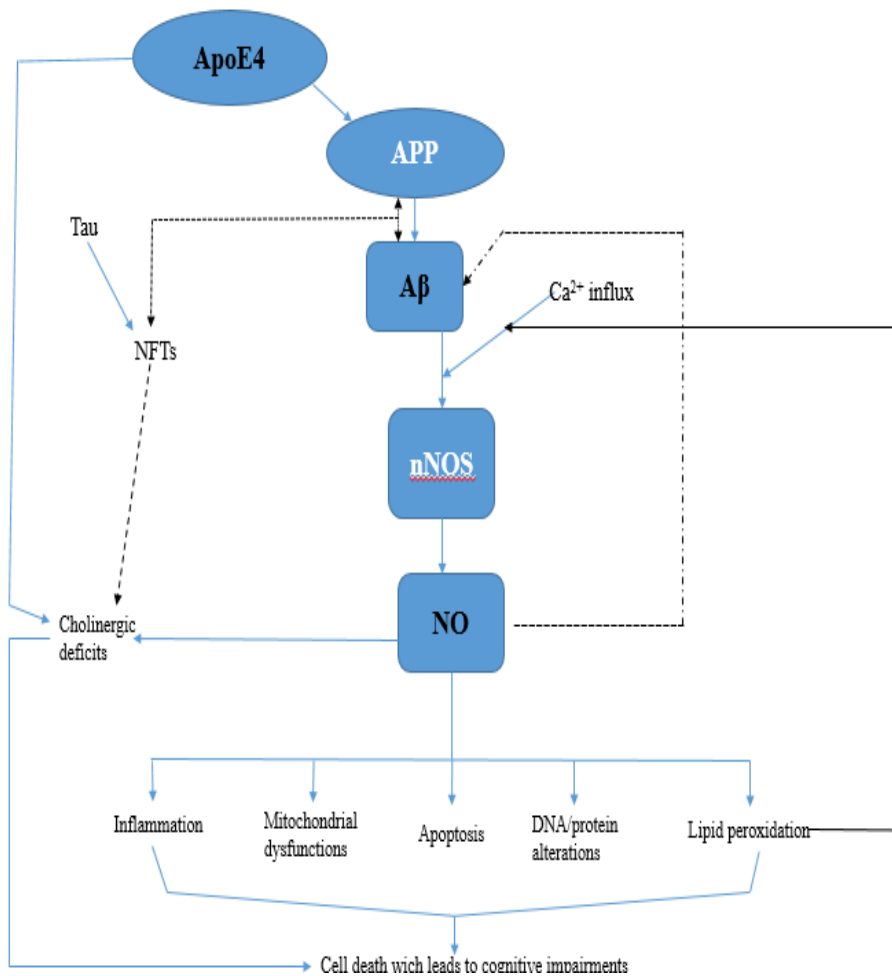


Figure 1.4: Diagram showing nitric oxide (NO) neurotoxicity in relation to AD.

NFT formation may influence A β accumulation and vice versa that leads to cell death secondary to disruption of cellular trafficking. Cholinergic deficit is one of the most significant findings in AD, and is implicated in memory impairments observed in this disease. Increased production of A β induces NO production either by disrupting Ca²⁺ homeostasis and subsequent increase in intracellular Ca²⁺ (nNOS and eNOS-mediated NO release) or by interactions with glial cells. These reactive oxygen species induce a variety of neurotoxic mechanisms, including DNA/protein alterations, mitochondrial dysfunction, apoptosis, neuro-inflammation, and lipid peroxidation (which jeopardize cellular membrane integrity, which leads to further Ca²⁺ influx and NO release). These mechanisms are likely to be involved in cell death and memory impairments observed in AD (Cetin, 2013).

Neuronal death in AD may result directly and/or indirectly from the triggering insults caused by A β toxicity, glutamate excitotoxicity, long-lasting oxidative stress, DNA damage, and elevation of intracellular Ca²⁺ levels. Thus, the mode of cell death in AD remains a matter of

controversy, and it is possible that both apoptotic and non-apoptotic cell death coexist in the brains of affected patients.

1.10 Manifestations of AD

Depending on the subtype of the disease, manifestations may either include or lead to behavioural changes or vascular diseases (Breteler, 2000). The amyloid cascade hypothesis suggests that early aggregation of A β triggers a complex of pathological cascades that lead to neurodegeneration with loss of working/short term memory as early symptoms (Fen et al., 2010) of disease manifestation. Methionine residue number 35 (Met 35) and neighbouring residues of A β are apparently important in this early aggregation (Pratim Bose et al., 2009). On the other hand, the cholinergic hypothesis proposes that it is the decrease in synthesis of the neurotransmitter acetylcholine that is the cause of AD (Bayer and Wirths, 2010).

In the vast majority of late-onset SAD, the majority of evidence collected does not support the amyloid cascade hypothesis as it is considered too narrow to explain all of the molecular mechanisms that lead to the characteristic accumulation of the neuropathological hallmarks of the disease (Simic et al., 2009). It is therefore not surprising that treatments aimed at lowering A β aggregation and production failed to show clinical improvement in AD patients. It is therefore necessary to gain a better understanding of the molecular and cognitive effects of different A β forms (Sipos et al., 2007) in order to design better therapeutic interventions targeting the A β cascade.

AD affects people differently. The most common symptom found among all patients is forgetfulness of new information. Over time, the disease progresses and reaches an irreversible level where the patient is unable to perform basic daily life activities such as bathing, dressing or eating (Mandell and Green, 2011). At the late stage of the disease, the patient cannot even move, communicate or recognize family members. The Patient then becomes vulnerable to infection which may be fatal. Clinically AD is characterized by cognitive decline and memory loss (Allison et al., 2001). Although mild cognitive impairments (MCI) represent the harbinger signs of the disease, patients with MCIs do not always develop AD. The presence of A β plaques in the cortex and NFTs mark the advanced level of AD (Madsen et al., 2010). Biochemical events including loss of neurons and

synapses in specific regions of the brain lead to the development of the disease and these are life-threatening.

1.11 Diagnosis

Historically diagnosis of AD was made after exclusion of all other possible causes of dementia, including metabolic imbalances such as vitamin deficiencies or other neurological disorders with more definitive diagnostic criteria (Findeis, 2007). Problems associated with AD and other neurodegenerative disorders arise from the fact that cognitive tests currently used to assess clinical benefit of symptomatic drug treatment might suffer subjectivity and little sensitivity to subtle changes over time (Deguil et al., 2013). The other problem is that no equivalent task exists for research animal models as the verbal component, which is primarily used in these tests, is lacking in animals (Deguil et al., 2013).

A clinical diagnosis of AD is made when patients have progressive memory decline for over 6 months with resultant impairment of self-care and social or occupational functioning (Chu, 2012), but this is still limited to probable or possible AD (Findeis, 2007). The presence of objective memory impairment should be documented by the Mini-Mental State Examination (MMSE) and other neuropsychological tests (Chu, 2012). Diagnosis of definite AD continues to require postmortem histological analysis of the brain to document the presence of characteristic senile plaques and tangles that define the disease (Findeis, 2007). The importance of the $A\beta_{40}/A\beta_{42}$ ratio emerged in examinations of both CSF and plasma of humans with or without AD and other neurodegenerative diseases (Findeis, 2007). Unlike other diagnostic methods that image brain function and/or volume, the $A\beta_{40}/A\beta_{42}$ ratio offers an opportunity to identify individuals at an even earlier pre-symptomatic stage of the disease (Findeis, 2007). Such individuals could then be placed on therapy that can potentially slow or prevent disease progression at a stage of disease where the efficacy of the treatment can be expected to be much greater than in patients at a more advanced stage of the disease (Findeis, 2007).

Other essential diagnostic points include deficits in two or more areas of cognition, absence of disturbance in consciousness, disease onset between the ages of 40 and 90 years, absence of systemic disorders or other brain diseases that could account for the progressive deficits in memory and cognition, evidence of cerebral atrophy on computed tomography (CT) or

magnetic resonance imaging (MRI) scans without other significant organic lesions, and the absence of any metabolic disorder.

1.12 Conventional management strategies

Current therapies of AD are merely palliative and only slow down cognitive decline. Treatments which address underlying pathologic mechanisms are completely lacking. Regular exercise, higher education and proper diet have been reported to be protective, as has smoking, despite its other negative health effects (Findeis, 2007). Other experimental therapies include vaccinations, secretase inhibitors and anti-inflammatory drugs (Behl and Moosmann, 2002).

Symptomatic relief that is provided by approved AD pharmacotherapies are lost with time and the disease progresses despite continued treatment (Farlow et al., 2010). Table 1 below, shows some of the approved acetyl cholinesterase inhibitor (AChEI) drugs for symptomatic relief of AD, however there remains a continued need for the investigation of more robust management strategies.

Table 1: Symptomatic drug treatments for Alzheimer’s disease

Drug	Class	Dose (mg/day)	Frequency (times/day)	Absorption affected by food	Metabolism
Donepezil (Aricept)	Cholinesterase inhibitor	5-10 [†]	1	No	CYP2D6 CYP3A4
Rivastigmine (Exelon)	Cholinesterase inhibitor	3-12	2	Yes	Non-hepatic
Galantamine (Reminyl; Reminyl PR*)	Cholinesterase inhibitor	8-32	2 1 (PR)	Yes	CYP2D6 CYP3A4
Memantine (Ebixa)	NMDA**-receptor antagonist	5-20	2 (one)	No	Non-hepatic

PR* denotes prolonged release, and NMDA** N-methyl D-aspartate. Table adapted from Chu (2012).

A β fibrillar and oligomeric forms have been shown to have neurotoxic effects *in vivo* and *in vitro* consequently strategies to prevent the formation of or to lower levels of A β in the brain are anticipated to be of tremendous therapeutic benefit. There are several AD immunotherapies that are currently under research which include, direct immunization with synthetic full length forms of A β and the administration of modified A β fragments that may be conjugated to specific carriers in order to stimulate T- and β -cell lymphocytic immune responses and evade challenges that accompany intensifying a T-cell reaction precisely against A β (Morgan, 2006, Delrieu et al., 2012).

Short peptides (<100 AAs) are the key regulators in a variety of biological activities because they offer high specificity associated with low toxicity and thus peptide beta sheet breakers (BSBs) have gained a lot of popularity because of these properties (Funke and Willbold, 2012). Several peptide based inhibitors or BSBs of the A β self-aggregatory process have been reported (Pratim Bose et al., 2009). The first pentapeptide BSB was reported by Tjernberg et al. (1996). Since then, these pentapeptide BSBs have demonstrated their efficacy *in vitro* and *in vivo* (Hetényi et al., 2002). There are a total of 67 therapeutic peptides on the market today, 150 are in clinical phases and there is more than 400 in the pre-clinical trial stages (Funke and Willbold, 2012). Principally short *N*-methylated peptides analogous to parts of the hydrophobic central region (residues ~16-24) of A β have been used to design these anti-amyloid factors or BSBs with attractive pharmacological properties (Pratim Bose et al., 2009, Sigurdsson et al., 2000). Figure 1.5 shows research directions and strategies in the search for AD-modifying drugs.

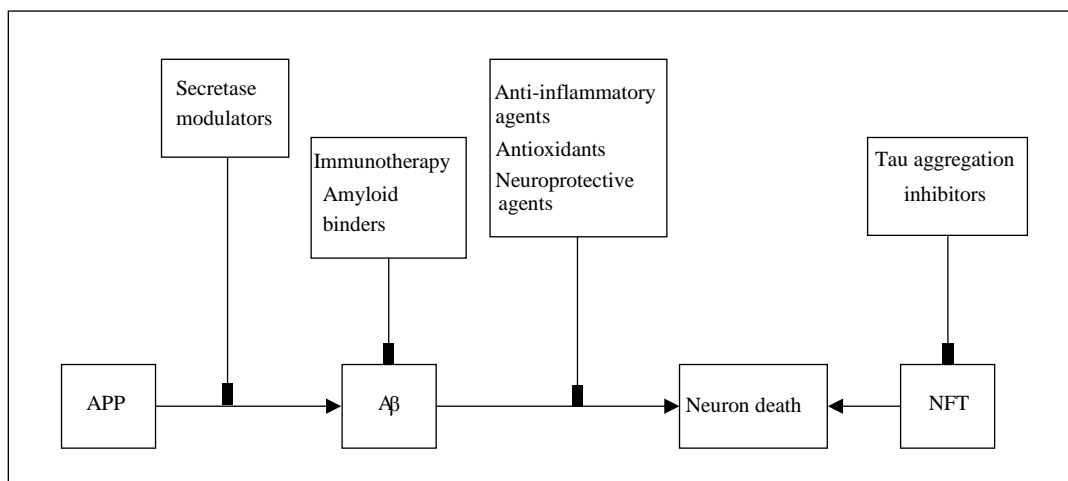


Figure 1.5: Research directions and strategies in the search for disease-modifying drugs
 APP denotes amyloid precursor, A β denotes beta-amyloid, and NFT neurofibrillary tangles (Chu, 2012).

While the central region of A β has attracted much attention, the C-terminal region has been far less explored despite the fact that this region forms intermolecular β -sheet contacts in A β fibrils and was previously proposed to be the kinetic determinant of the self-assembly process (Pratim Bose et al., 2009). More recently it was also demonstrated that peptides derived from A β positions 28-42 were efficient in protecting neurons from A β toxicity, again pointing to the importance of the C-terminal region (Pratim Bose et al., 2009).

1.13 Poly - N - methylated Amyloid - β - Peptide (A β) C - terminal Fragments (MEPTIDES)

In a recent study a novel compound Poly - N - methylated Amyloid - β - Peptide (A β) C - Terminal Fragments (MEPTIDES) (Figure 1.6) was shown to reduce A β toxicity *in vitro* and in *Drosophila melanogaster*. This study found that the C - terminal fragments (covering residues 31 - 42 or parts thereof) may be incorporated into the putative hydrophobic core of A β oligomers consequently disrupting it and thereby reducing its toxicity (Pratim Bose et al., 2009). However whether this novel drug is equally effective in mammals to inhibit A β - induced toxicity remains unknown.

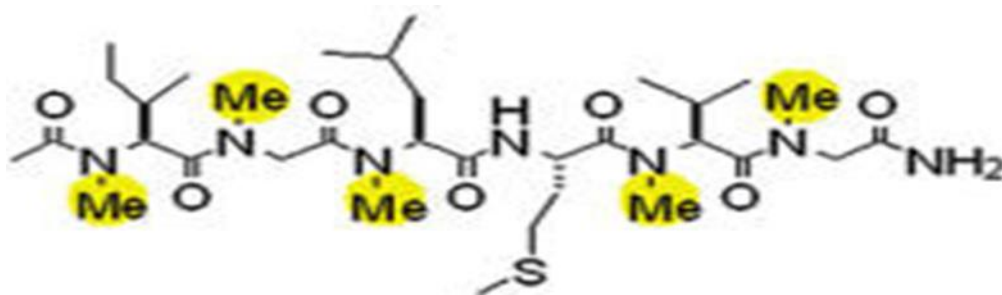


Figure 1.6: Diagram showing Molecular structure of MEPTIDES. Image adapted from Pratim Bose et al. (2009).

1.14 Basis of the study

As stated earlier, the prevention and/or retardation of progressive AD, will have substantial medical, social and financial benefit to the patient, family members and the entire health care fraternity. We hypothesized that MEPTIDES will reverse the neurotoxic effects of $A\beta_{42}$ *in vivo*.

1.14.1 Aims

The aims of the present study were therefore to

- Establish and characterize a rat model that may resemble some of the symptoms of AD; and to
- Evaluate the efficacy of MEPTIDES *in vivo* as a possible anti-AD drug.

CHAPTER 2

Materials and Methods

2.1 Materials and methods

2.1.1 Reagents and materials

A β ₄₂ peptides were purchased from DLD Scientific and MEPTIDES were synthesized by manual solid phase peptide synthesis on a Sieber resin with HATU as coupling reagent (Pratim Bose et al., 2009) by the University of KwaZulu-Natal Catalysis and Peptide Research Unit. OxiSelect™ ZR RNA MiniPrep™ kit was purchased from Zymo Research CORP. Nano-drop® ND-100 Spectrophotometer (Thermo Scientific, SA) was used for detection of RNA purity. iScript™ cDNA Synthesis Kit (Bio- RAD, SA), primers designed and produced commercially (Inqaba, SA) were used to synthesize cDNA. Fast Start SYBR Green I, Gene-Amp 9700 Thermocycler from (Applied Biosystems, California, USA) and Light Cycler and software 4.1 (Roche Diagnostics) were used for qPCR caspase-3 gene amplification and analysis of results. OxiSelect™ HNE Adduct Immunoblot kit (Cell Biolabs Inc) was used to measure 4HNE levels. Labotec Titramax 1000 orbital shaker was used to in all steps that required shaking. Odyssey CLx, blocking buffer, IRDye from (LiCOR Biosciences) were used in western blotting. Anti-rabbit IgG HRP-linked (Cell Signaling Technology) and Chemi-doc system used was from (Bio-RAD, SA). Leica CM 1100 cryostat was used to cut brain sections. MALDI-TOF Autoflex III™ Speed MS, software Flex Imaging 3.0, ImagePrep station and Indium-tin-oxide (ITO) type I slides (Bruker Daltonics, Germany) were used to determine MEPTIDES distribution in the brain.

2.1.2 Ethical clearance

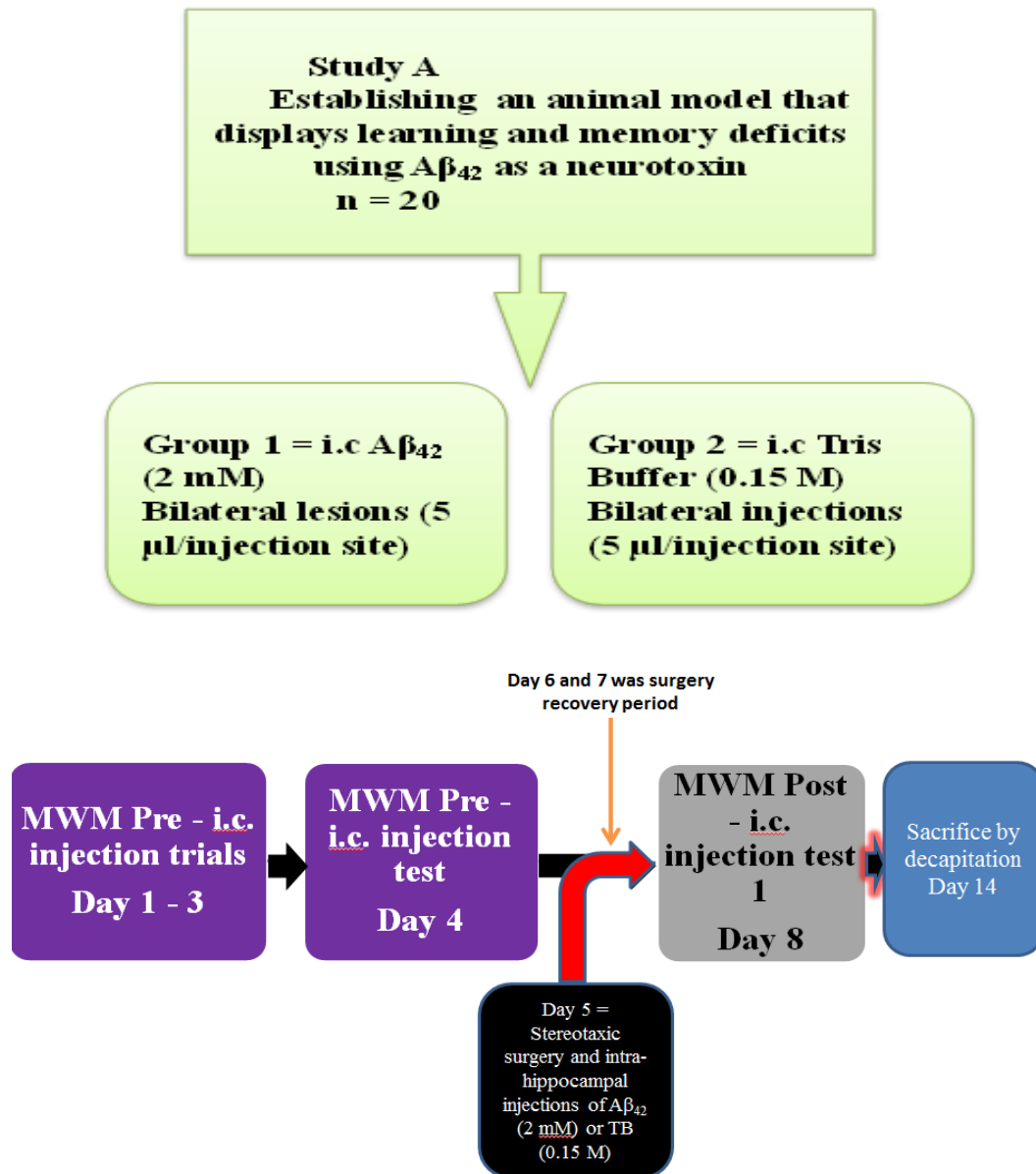
Ethical clearance was obtained from the University of KwaZulu-Natal Ethics Committee. The reference number is 048/13/Animal. Institutional guidelines for animal care were followed (Animal Ethics Committee of the University of KwaZulu-Natal, 2007). All efforts were made to minimize animal suffering and to reduce the number of animals used.

2.1.3 Animals

Fully grown male Sprague-Dawley (SD) rats (n = 40) weighing between 300 – 350 g (8/9 weeks of age), at the beginning of the study, were used. The rats were randomly assigned to 4 groups (n = 10 rats/group) and housed under standard lighting conditions (12 hour light/dark cycles) (Sipos et al. , 2007), lights on at 06:00, 25 °C room temperature, humidity of 70%, at the Biomedical Resource Unit, University of KwaZulu-Natal, Westville campus. Food and water was available *ad libitum*.

2.2 Experimental design and timeline

Study A



Study B

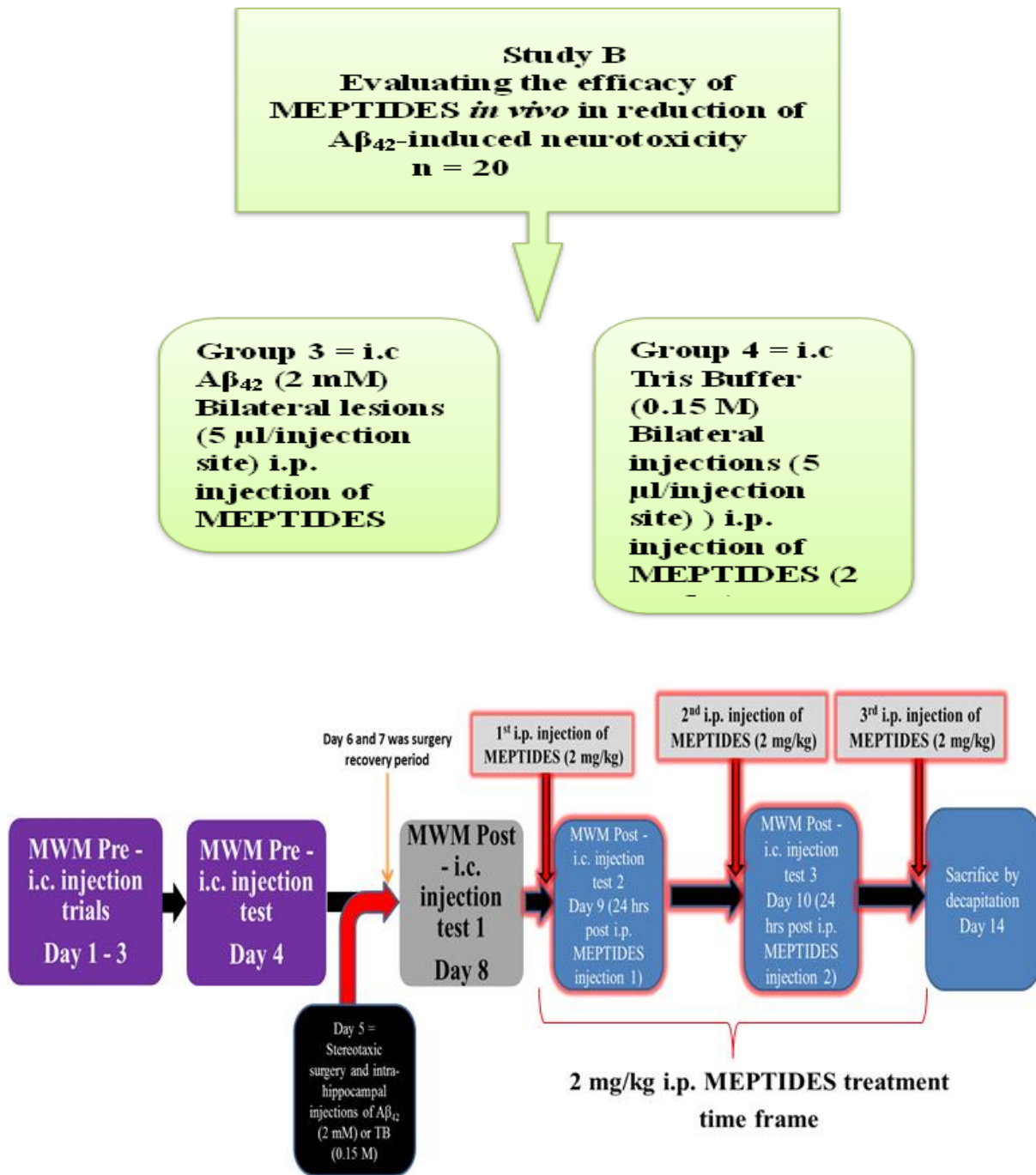


Figure 2.1: Diagram showing experimental design and timeline for study A and B.

2.3 Stereotaxic surgery

On day 5, the rats were first given atropine (0.1 mg/kg, i.p.) and subsequently anaesthetized using sodium pentobarbital (60 mg/kg, i.p.). After full anaesthesia (the absence of hind paw reflex) was achieved, the head was shaved and the rat was placed in a stereotaxic apparatus (David Kopf Instruments, CA, USA). A midline sagittal incision was made on the scalp and the underlying tissue removed to expose the skull. Burr holes through which the injecting needles were pushed into the brain, were drilled through the skull at the following coordinates: Anterior - Posterior = -4.8 mm from bregma; Medio-Lateral = ± 3.4 mm from the midline suture; and depth of 3.0 mm below the dura according to the Atlas of Paxinos and Watson (5th Edition, 2005). A β_{42} (2 mM) or Tris buffer (TB 0.15 M) (Shin et al., 1997) was injected bilaterally into the dorsal hippocampus using a Hamilton syringe which had been pretreated with dimethyldichlorosaline to prevent the A β_{42} from adhering to the inner surface of the syringe, at a rate of 1 μ l/minute for 10 minutes to deliver a final volume of 10 μ l. A further 2 minutes was allowed for optimal diffusion of the drug into the brain. The burr holes were closed with bone wax and the wound was sutured and cleaned with iodine solution. Cellulose was used for the dressing of the wound (Purdue Frederic, USA). The rats were placed on a heating blanket to prevent hypothermia during surgery. They were returned to their home cages after full recovery from surgery. The rats were then given a 2-day recovery period. The rats were handled and weighed each day during this recovery time. Subsequent to the recovery period, on day 8, the rats underwent spatial learning and memory tests in the Morris water maze.

2.4. Learning and Memory tests



Figure 2.2: Diagram showing Morris Water Maze tank.

The Morris water maze is a circular tank/maze 1 m in diameter with 4 imaginary quadrants. The level of usually opaque water (temperature between 22 - 25°C, to minimize hypothermic stress of the rat) was just high enough to cover the top of a clear Perspex platform (10 x 10 cm wide and 20 cm high). The platform was placed in one of the quadrants, while the rat was placed in any of the other 3 quadrants. The rat was given 2 minutes to find its way to the platform. If not, the rat was gently guided to the platform during training after the 2 minutes had expired, and once on the platform the rat was given a maximum 15 seconds to familiarize itself with the position of the platform within the maze. There were 3 different starting positions, selected pseudo-randomly, at the borders of the quadrants in the tank. The rationale of the test is that the animal needs to find the platform using its memory of constant spatial cues placed around the maze.

There were 3 training sessions, done on 3 consecutive days, with a pre - i.c. injection test on the 4th day, following the final training session. The post-injection tests started 2 days after the i.c. injections of either TB or A β ₄₂. On day 8, post-lesion test 1 was performed. On days 9 and 10, post-lesion tests 2 and 3 were carried out and the rats also received a MEPTIDES or saline injection (i.p.) after each test. The parameter that was recorded was the time taken for the rat to reach the hidden platform during all trials and tests. The rats were sacrificed on day 14 by decapitation.

2.5 Sacrifice

After completing the behavioural experiments, the animals were decapitated on day 14 (between 10 am and 1 pm). Three whole brains from the MEPTIDES-treated A β ₄₂ and TB groups were rapidly removed from the skull placed in containers and gently immersed in liquid nitrogen until frozen. The brains were slowly immersed in the liquid nitrogen in order to preserve the morphology of the brain tissue. The hippocampus was dissected out of fresh brains in all the other the animals. Dorsal and ventral hippocampi were weighed, placed in Eppendorf vials and snap frozen in liquid nitrogen. The samples were then stored for a maximum of one month in a biofreezer at a temperature of -73 °C for further biochemical analysis.

2.6 Biochemical Assays

2.6.1 Real time PCR

Total ribonucleic acid (RNA) was isolated from previously stored snap frozen hippocampal tissue. The hippocampal tissue weighing between 20-50 mg was homogenized in 400 μ l of RNA lysis buffer using a sonicator (12000 Hz for 10 seconds). The RNA was extracted as per manufacturer's instructions. The purity of the RNA was determined using a Nano-drop® ND-100 Spectrophotometer with the purity of RNA determined by the absorbance ratio at 260 nm/280 nm. RNA was considered pure if the absorbance ratio ranged between 1.7 and 2.5. The isolated RNA was used to synthesize cDNA using the iScript™ cDNA Synthesis Kit, as per manufacturer's instruction. The RNA was converted to cDNA using the GeneAmp 9700 Thermocycler, with the following parameters: melting point 25 °C for 5 minutes, 40 °C for 30 minutes, 85 °C for 5 minutes and hold at 4 °C. The cDNA was then stored at – 20 °C until further analysis. The primers and their sequence are shown in Table 2. The expression of caspase-3 (C3) gene was subsequently assessed using a Light Cycler. The Light Cycler-master mix consisted of the following: 5.4 μ l water, 1.6 μ l MgCl₂ (3 mM), 1.0 μ l forward primer (1.0 μ M), 1.0 μ l reverse primer (1.0 μ M), 1.0 μ l Fast Start SYBR Green I, and 1.0 μ l cDNA. RNA was quantified using the Light Cycler under the following PCR conditions: one cycle consisted of 95 °C for 10 minutes followed by 45 cycles at 95 °C for 15 seconds, 60 °C for 1 minute and 72 °C for 10 seconds using a single fluorescence measurement (Mackraj et al., 2008, Zhu et al., 2011). This was followed by a final cooling

step to 40 °C. A dilution series of C3 gene and GAPDH amplicons were used to construct a standard curve. Quantitative analysis of the data was performed using Light Cycler software 4.1. Melting curve analysis was done to detect the presence of a single specific product.

Table 2. Sequences of primers for real-time qPCR (Inqaba, SA)

Target gene Primers (5'-3')	(nt ¹)	PP ²	Bp ³
Caspase-3 F5'-GGTGCCACTATGAATTTGAAATTAC-3'	25	1216-1240	25
R5'-CCAACTCTTCATTTCCACAG-3'	20	1401-1382	20

¹ length, ² primer position, ³ product size.

2.6.2 ELISA

TNF- α was quantified using a sandwich ELISA from previously stored snap frozen hippocampal tissue. The hippocampal tissue of 5 animals per group (A β ₄₂, TB) weighing between 20-50 mg was homogenized in 600 μ l of RIPA buffer (see Appendix B). Homogenates were centrifuged twice at 3578 g for 10 minutes at 4 °C. Supernatant was collected and protein concentration determined using the Bradford method (see Appendix A for standard curve and Appendix B Bradford method protocol) (Kruger, 2009). The protein lysate was stored at -80 °C after protein determination and standardization of protein concentration. Sample supernatant (diluted 5-fold) or protein standard (100 μ l) were added to each well and incubated for 2.5 hours in the dark at 4 °C with gentle shaking on an orbital shaker. Plates were then washed 4 times with 1 X wash buffer (300 μ l) using a multichannel pipette. Biotinylated anti-rat TNF- α antibody (100 μ l) was added to each well and incubated for 1 hour at room temperature with gentle shaking on an orbital shaker. Plates were washed again 4 times with 1 X wash buffer (300 μ l) using a multichannel pipette. HRP-conjugated streptavidin (100 μ l) was added to each well and incubated for 45 minutes at room temperature with gentle shaking on an orbital shaker followed by 4 washes with 1 X wash buffer (300 μ l) using a multichannel pipette. Hundred microliters of 3, 3', 5, 5'-tetramethylbenzidine (TMB) substrate solution was added for 30 minutes at room

temperature in the dark with gentle shaking. Finally, 50 μ l of stop solution was added to each well and absorbance was measured at 45nm on a plate reader.

2.6.3 Western Blotting

The hippocampal tissue of 4 animals per group from the A β ₄₂, TB, MEPTIDES-treated A β ₄₂ and MEPTIDES-treated TB groups, was homogenized in 600 μ l of RIPA buffer (see Appendix B). Homogenates were centrifuged twice at 3578 g for 10 minutes at 4 °C. Supernatant was collected and protein concentration determined using the Bradford method (Appendix B) (Kruger, 2009). The protein lysate was stored at -80 °C. After protein determination and standardization of protein concentration, equal amounts of protein samples (40 μ g) were diluted at a ratio of 1:2 with Bio Rad sample buffer (Appendix B). The mixture was heated at 95 °C for 5 minutes. The electrophoresis apparatus was set up and filled with running buffer (Appendix C). The protein samples were loaded onto the gel (30 μ g protein in each well). (Note: The volume of protein samples varied to obtain similar amount of protein in each well). The samples were run on the SDS-PAGE gel at constant 200 Volts and fluctuating current (between 1 - 400 mA) for 45 to 50 minutes or until the bottom most marker band reached the bottom of the gel. Proteins separated on the gels were then transferred to nitrocellulose membranes using the traditional transfer method, with constant current (400 mA) and variable voltage (between 1 - 250 V). Transfer required 60 minutes with this method. The membranes were subsequently blocked in non-fat milk (Appendix C) or blocking buffer (LiCOR Biosciences), for 2 hours. Membranes were then incubated overnight at 4 °C with either C3 or 4HNE primary antibody in 0.2 % Tween 20 in Tris buffered saline (TBS-T)/blocking buffer (1:1000), after which they were washed three times (5 minutes each wash) with TBS-T. The membranes were washed with 0.2 % Tween 20 in Phosphate buffered saline (PBS-T) if they were going to be viewed on the Odyssey CLx. The membranes were then incubated with anti-rabbit IgG HRP-linked or IRDye antibody as the secondary antibody (1:10000 or 1:150000 respectively) for 2 hours and washed twice with TBS-T or PBS-T and finally with TBS or PBS. Membranes viewed on the Odyssey CLx were viewed immediately after the final wash step. The chemiluminescence peroxidase substrate-3 reagents were added to the membranes that were viewed on the Chemi-doc system. Densitometric values were normalized to β -actin.

2.6.4 MALDI -TOF

Previously stored whole brain samples of naïve control, and MEPTIDE-treated TB- and A β ₄₂-injected rats were sectioned using a cryostat (Leica CM 1100) into 10 μ m thick sections and were placed onto chilled ITO coated MALDI TOF slides. The sections were then desiccated for 24 hours to remove any air bubbles.

2.6.4.1 MALDI IMS matrix conditions

For manual spotting, a-cyano-4-hydroxycinnamic acid (CHCA) was prepared in 50:50:0.1 acetonitrile (ACN)/H₂O/trifluoroacetic acid (TFA) under saturated matrix conditions. The drug (MEPTIDES) standard was mixed (1:3) with CHCA matrix solution and 0.5 ml were placed onto a MALDI target (steel plate) or a control tissue for analysis. Matrix solution without the analyte was placed on tissue sections as control to check for matrix derived peaks interfering with the mass of the drug.

For the imaging MALDI MS experiments, the tissue sections were coated with CHCA matrix solution using an automatic spraying device (Image Prep, Bruker Daltonics). The Image Prep instrument deposits matrix solution onto the tissue in a controlled manner. Briefly, a matrix aerosol is created by vibrational vaporization under controlled conditions with all droplet diameters \leq 50 μ m and an average droplet size of \approx 20 μ m. A modified customized method was used for matrix application using the ImagePrep instrument. The parameters for incubation time, wetness and matrix thickness were optimized to get the best spectra possible without delocalization of drug or endogenous compounds on the tissue. The thickness of the matrix layer was monitored by the output from the optical sensor. In short, the method contained four identical phases in which a matrix layer corresponding to 0.3 V was added by repeating a spray cycle of 2.5 s followed by 10 s incubation time and 90 s of drying time (influx of N₂). The coated tissue sections were dried in the desiccator for 20 minute before analysis.

2.6.4.2 MALDI IMS detection limits and MS/MS verification

The range of detection was investigated by applying different concentrations of the MEPTIDES onto a control brain section. The MEPTIDES was mixed (1:3) with matrix solution and the different amounts of the analyte applied to the tissue in a total volume of 0.5 μ l. The matrix spots were analyzed in reflectron mode collecting 200 shots per spot. Using MS mode, the peptide was detectable down to 1 ng and the signal response was 8 arbitrary units (au). The MEPTIDES standard was also analyzed in MS/MS mode using a LIFT method. The LIFT method was calibrated on the CHCA matrix peak of 379.1 Da and its fragments. The same method was used to perform MS/MS directly on naïve control, MEPTIDES-treated TB-injected and MEPTIDES-treated A β ₄₂-injected brain tissue and spectra generated were compared. Using the MS/MS mode, the MEPTIDES was detectable down to 1 ng.

MS experiments were carried out using the AutoFlex III MALDI-TOF MS equipped with a solid-state Smartbeam laser operating at 200 Hz. The MS spectra were acquired in positive reflectron mode. For the initial analyses of the manually deposited spots, spectra consisting of 1000 laser shots were acquired in bundles of 5 x 200 shots and data were collected between m/z 200 - 800 Da. Prior to analysis the MS method was calibrated using a standard peptide mix (Bruker Daltonics, Germany) and the matrix cluster peak from CHCA at m/z 379.1 Da. The MS/MS experiments were performed using a LIFT method optimized for the MEPTIDES by specific tuning of the timing of the LIFT cell and of the precursor ion selector.

The software Flex Imaging 3.0 was used to set up the acquisition of the imaging experiments. The imaging MS experiments were performed by collecting spectra (200 shots) at a resolution of 200 μ m in the same m/z range as above.

The spectra were baseline subtracted (Convex hull) and smoothed (Savitzski golay) in the processing software during acquisition. In MS/MS mode, all spectra were normalized against root mean square (RMS) to reduce the influence of matrix hot spots. Here, we define the RMS as the root mean square of all spectra in the mass range analyzed. In this mode, both fragments and parent spectrum were acquired from each spot and 500 laser shots were summed up in a random walk pattern from each position.

2.7 Data presentation

All results are presented as mean \pm SEM. Software program Graphpad Prism (version 5.0, San Diego, California, USA) was used to analyze all statistical data. Data were subjected to either ANOVA with repeated measures where appropriate, followed by Bonferroni's posthoc test or non - parametric methods that included the Kruskal-Wallis and Mann-Whitney U tests. The t-test was used to test for a significant difference between two groups. The p value that was less than 0.05 was considered significant.

CHAPTER 3

Results

Study A

3.1 Behavioural results

All rats were subjected to three days of learning trials and a pre- i.c. injection test was performed on day 4. The rats then received bilateral injections (10 μ l, i.c.) of either Tris buffer (TB 0.15 M) or A β ₄₂ (2 mM) directly into the dorsal hippocampus. A 2-day period of recovery was allowed subsequent to the i.c. injections. The rats then underwent post- i.c. injection tests in the same MWM to determine the integrity of memory of the rats. All rats showed good learning ability before the i.c. injections (this was when trial 1 was compared to the pre- i.c. injection test using repeated measures ANOVA of the latency to reach the hidden platform), see Appendix A.

The ANOVA showed that there were significant differences between groups ($F_{(3, 36)} = 4.00$, $p = 0.01$, Figure 3.1 $n = 10$ /group). Bonferroni's posthoc test showed that there was a significant difference in time taken to find the hidden platform in the MWM when the A β ₄₂ pre-injection test was compared to A β ₄₂ post-injection test (18.20 ± 7.28 vs 49.60 ± 10.22 , $p < 0.05$). The time taken to find the hidden platform by the A β ₄₂ group post- i.c. injection of A β ₄₂ was also significantly different from the TB post-injection test (49.60 ± 10.22 vs 16.10 ± 4.22 , $p < 0.05$), (Figure 3.1).

Sixty percent of the rats in the TB-injected group showed decreased time to reach the hidden platform vs 80 % of the rats in the A β ₄₂-injected group who showed an increased time to reach the hidden platform in the MWM when the post- i.c. injection test was compared to the pre- i.c. injection test of the same rats in their respective groups (Figure 3.2 A and B).

The first aim of the present study was to establish and characterize a rat model that may resemble some of the symptoms of AD. We now had face validity through the MWM behavioural results and we were confident that a single bilateral i.c. injection of A β ₄₂ (2 mM) into the dorsal hippocampus impaired spatial learning and memory in adult male SD rats.

Several hypotheses of mechanisms of the neurotoxic effects of A β ₄₂ exist; we investigated inflammation, oxidative stress and apoptosis to test these hypotheses in our model.

3.2 TNF- α ELISA results

Literature suggests that one of the earliest disruptions that occur in the brain following A β ₄₂ aggregation is the upregulation of inflammatory cytokines. TNF- α is one of the cytokines that has been observed to be upregulated in AD patients following A β aggregation (Johnstone et al., 1999, Akiyama et al., 2000). We performed an ELISA to determine the levels of TNF- α in the dorsal hippocampi of our TB- vs A β ₄₂-injected rats for validation of these previous findings in the present rat model of AD. The linear range for the ELISA is indicated in chapter 2 (2.5.2 ELISA). The t-test analysis of hippocampal TNF- α levels did not show any significant difference (5190 ± 186.70 vs 5032 ± 440.40 , $p > 0.05$) when the TB- and A β ₄₂-injected rats were compared (Figure 3.3).

3.3 4HNE Western blot results

It is unclear whether increased ROS production causes A β ₄₂ aggregation in the AD brain or vice versa, but there is certainty that disruption of the metabolic pathways of one of the ROS products has detrimental effects on the physiological homeostatic balance of an organism. We measured 4HNE levels in the dorsal hippocampi using Western blotting. 4HNE is a product formed when ROS react with the lipid bilayer of cell membranes. The aim was to determine whether oxidative stress was one of the mechanisms by which A β ₄₂ exerted its neurotoxic effects. The linear range and protein amounts used for the Western blots are indicated in chapter 2 (2.5.3 Western Blotting). The t-test showed that there was no significant difference between the A β ₄₂- and the TB-injected rats when the 2 groups were compared (4.60 ± 0.35 vs 4.30 ± 0.61 , $p > 0.05$), (Figure 3.4).

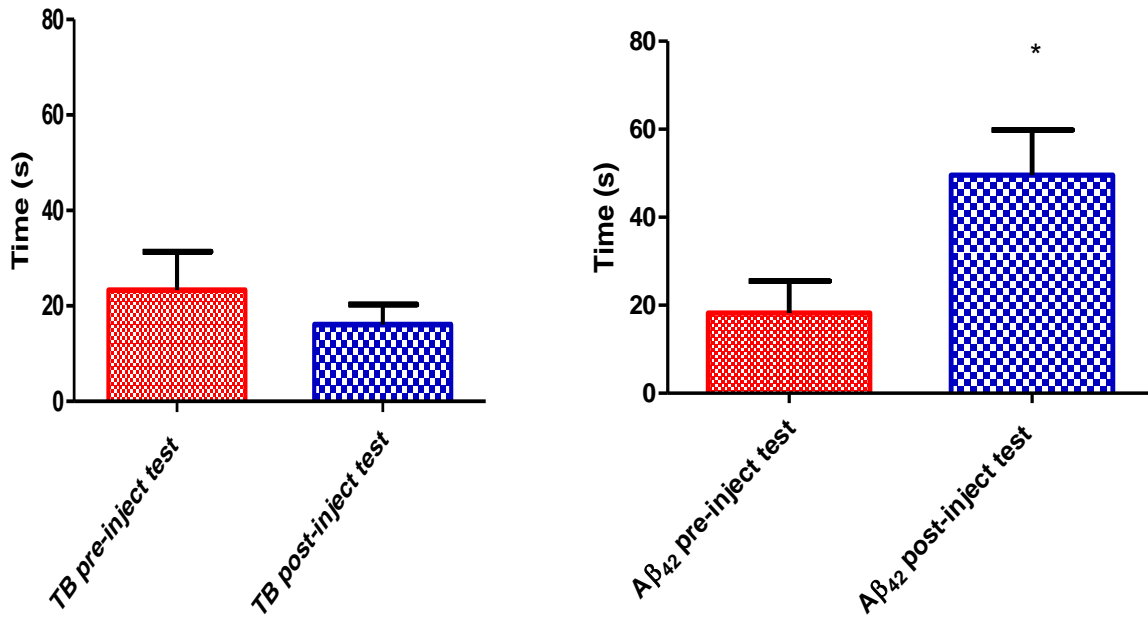


Figure 3.1: Graph showing time taken by TB-injected and Aβ₄₂-injected rats to find the hidden platform in the MWM. The pre-injection test is the test before the i.c injection of TB or Aβ₄₂ (10 μl, i.c., bilaterally) to create lesions similar to those observed in AD. The significant difference observed between the Aβ₄₂ pre-injection test vs Aβ₄₂ post-injection test (18.20 ± 7.28 vs 49.60 ± 10.22, *p < 0.05), shows a decrease in ability to recall the location of the platform in the rats injected with Aβ₄₂. The significant different observed when Aβ₄₂ post-injection test was compared to TB pre and post-injection tests (49.60 ± 10.22 vs 23.30 ± 8.07 and 49.60 ± 10.22 vs 16.10 ± 4.22, *p < 0.05), show that TB- i.c. injections did not impair recall ability of the control rats in the MWM.

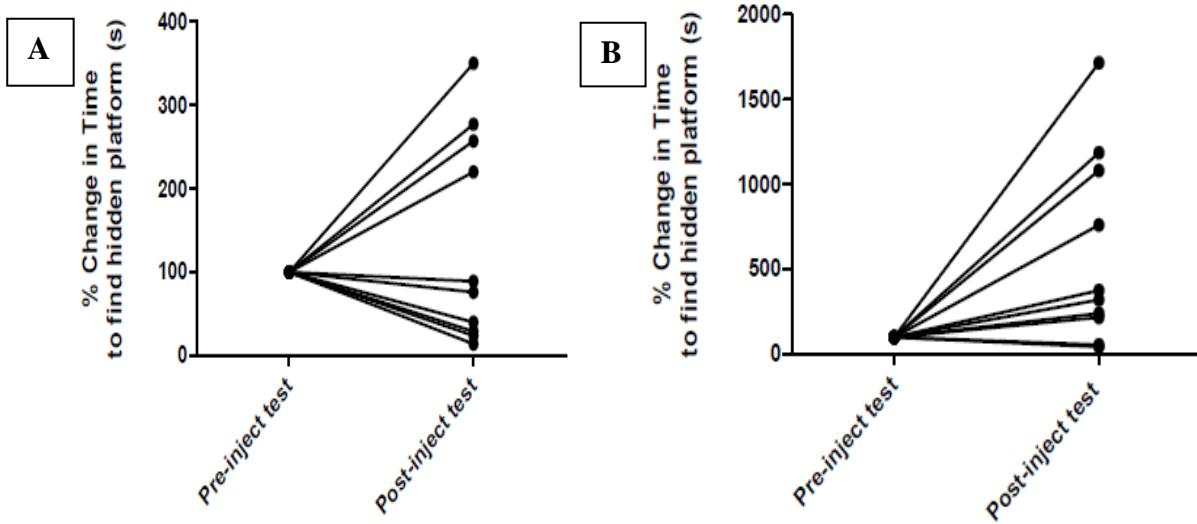


Figure 3.2: Diagram showing percentage change in the time taken to find the hidden platform in the MWM when the post- i.c. injection test of the TB- and A β_{42} -injected rats was compared to the pre- i.c. injection test of the same rats in their respective groups. The pre - injection test was taken as 100 % for all comparisons. Figure 3.2 A shows post- vs pre- i.c. injection test of the TB-injected rats. Sixty percent of the rats in this group showed decreased time to reach the hidden platform vs the 40 % that showed an increased time to reach the hidden platform. Figure 3.2 B shows post- vs pre- i.c. injection test of the A β_{42} -injected rats. Eighty percent of the rats in this group showed an increased time to reach the hidden platform vs 20% that showed a decreased time to reach the hidden platform.

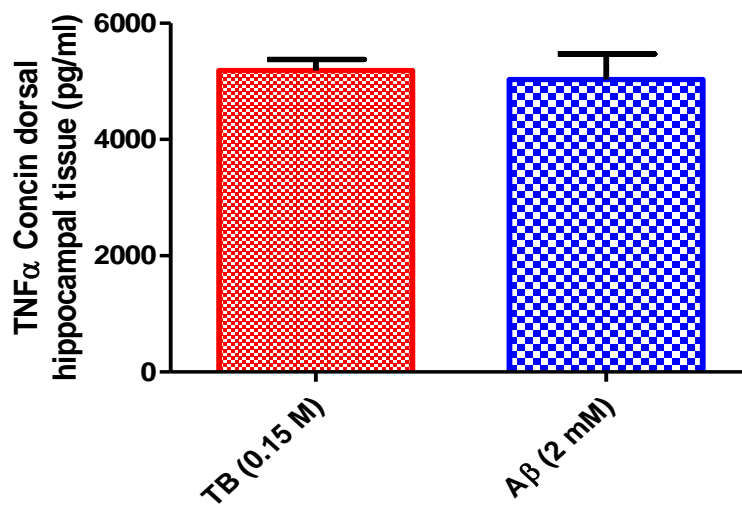


Figure 3.3: Graph showing expression of TNF- α in the dorsal hippocampus of TB vs A β_{42} -injected rats. The t-test analysis of our TNF- α results did not show any significant difference (519 \pm 186.70 vs 5032 \pm 440.40, $p > 0.05$) when the TB and A β_{42} -injected groups were compared.

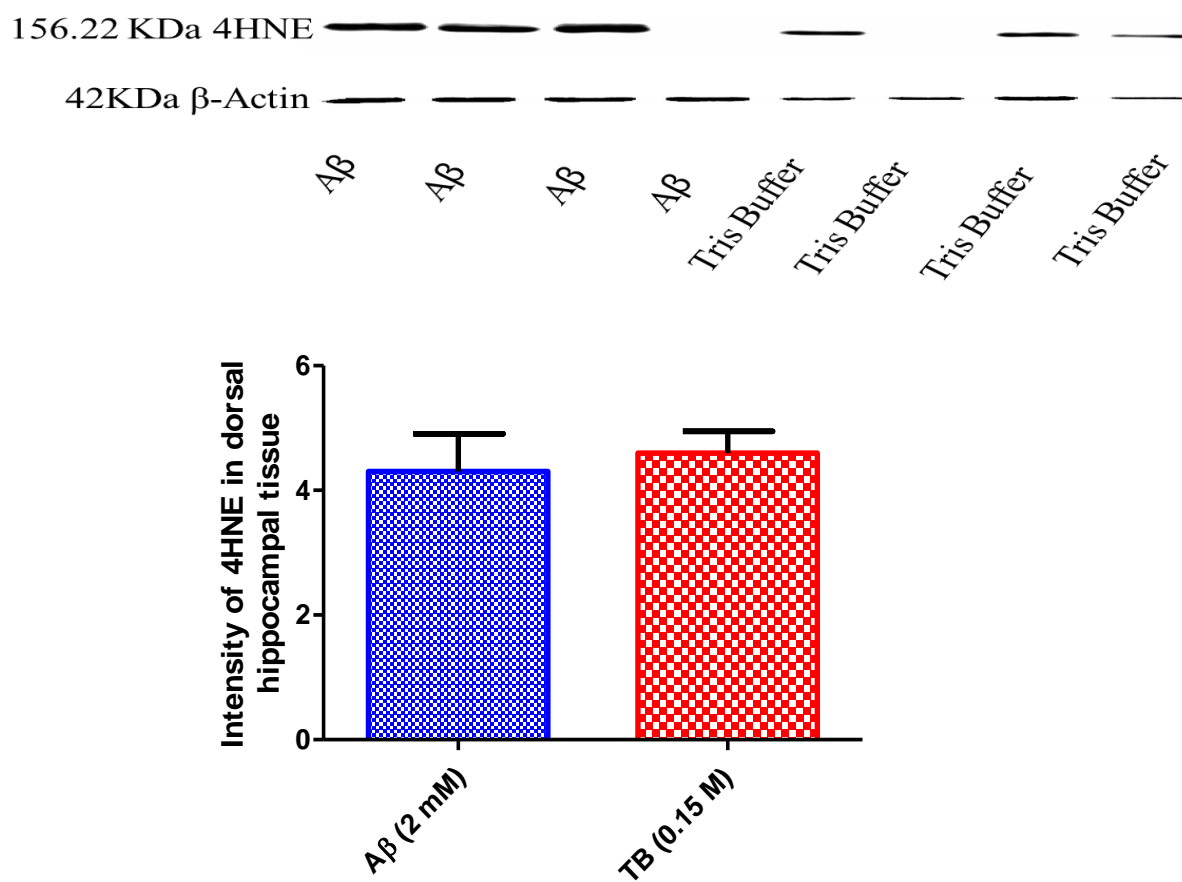


Figure 3.4: Graph showing 4HNE Western blot results obtained for the dorsal hippocampi of Aβ₄₂- vs TB-injected. The t-test analysis showed that there was no significant difference between the 2 groups (4.60 ± 0.35 vs 4.30 ± 0.61, p > 0.05).

Study B

3.4 Behavioural results

A similar trend was observed in the MEPTIDES-treated groups. The ANOVA showed a trend for the groups to be different from each other ($F_{(7, 69)} = 2.10$, $p = 0.05$, Figure 3.5 $n = 10$ /group). Bonferroni's posthoc test showed a significantly increased time to find the hidden platform in the $A\beta_{42}$ post-injection test 1, which is the first test before i.p. injection of MEPTIDES, compared to the $A\beta_{42}$ pre-injection test (17.60 ± 4.24 vs 56.00 ± 12.41 , $p < 0.05$). This time was significantly reduced 24 hours after the first MEPTIDES i.p. injection in the same group (56.00 ± 12.41 vs 21.50 ± 5.27 , $p < 0.05$), (Figure 3.5).

3.5 C3 qPCR results

There is extensive evidence to suggest that aggregation of $A\beta_{42}$ in susceptible brain regions causes cell death (Loo et al., 1993, Awasthi et al., 2005) which leads to a decreased number of functional synapses. In the cerebral cortex specifically, this is associated with the dementia that is observed in AD patients. One of the mechanisms of cell death caused by $A\beta$ is through activation of the caspase pathway (Cetin, 2013, Awasthi et al., 2005). We performed C3 gene qPCR and C3 protein Western blot analysis to test this theory in our model.

There was a significant difference between groups in C3 gene expression revealed by ANOVA ($F_{(3, 12)} = 13.14$, $p = 0.0004$). Bonferroni's posthoc test showed a significant upregulation of the C3 gene when the $A\beta_{42}$ -injected rats were compared to TB-injected rats (2.54 ± 0.45 vs 1.155 ± 0.11 , $p < 0.05$). Notably, C3 gene expression decreased significantly to baseline levels when $A\beta_{42}$ -injected rats were compared to MEPTIDES-treated $A\beta_{42}$ -injected rats (2.54 ± 0.45 vs 0.77 ± 0.04 , $p < 0.05$), (Figure 3.6).

3.6 C3 Western blots results

Western blot results for C3 protein levels in dorsal hippocampal tissue of TB-injected, A β ₄₂-injected, and MEPTIDE (2 mg/kg)-treated rats are shown in Figure 3.7 A and B. The linear range and protein amounts used in the Western blot are outlined in chapter 2 (2.5.3 Western Blotting). The t-test analysis of TB- vs A β ₄₂-injected rats did not show any significant difference in the dorsal hippocampal C3 protein levels (1.38 ± 0.09 vs 1.55 ± 0.27 , $p > 0.05$), (Figure 3.7 A). The t-test analysis of the MEPTIDE (2 mg/kg)-treated TB- vs A β ₄₂-injected rats also did not show any significant difference when the 2 groups were compared (0.19 ± 0.04 vs 0.11 ± 0.01 , $p > 0.05$), (Figure 3.7 B).

3.7 MALDI TOF MS results

MALDI TOF MS was performed on brain samples that were from the TB-injected + MEPTIDES-treated rats vs A β ₄₂-injected + MEPTIDES-treated rats to determine whether MEPTIDES cross the BBB and their abundance in the brain. Optimization was first done by spotting the MEPTIDES on the metal target plate (Bruker Daltonics, Germany) and a naïve rat brain (see Appendix D). The different methods used to obtain spectra are outlined in chapter 2 (2.5.4.2 MALDI IMS detection limits and MS/MS verification). Na⁺ adducts of MEPTIDES (722.41 ± 0.20 % m/z) or Na⁺/K⁺ adducts of fragments (674.12 ± 0.2 % m/z and 690.043 ± 0.2 % m/z) thereof were obtained. The Na⁺/K⁺ adducts of the fragments are indicated by a peak at 712.41 ± 0.20 % m/z (see Appendix D). The m/z values obtained from the optimization results were used to analyze experimental brain tissue. There was a greater abundance of the Na⁺/K⁺ adduct of the fragments in the MEPTIDES-treated A β ₄₂-injected rat brain (Figure 3.8 C) when it was compared to the MEPTIDES-treated TB-injected brain (712.41 ± 0.20 % m/z) (Figure 3.8 B). This peak was not observed in the control naïve brain (Figure 3.8 A).

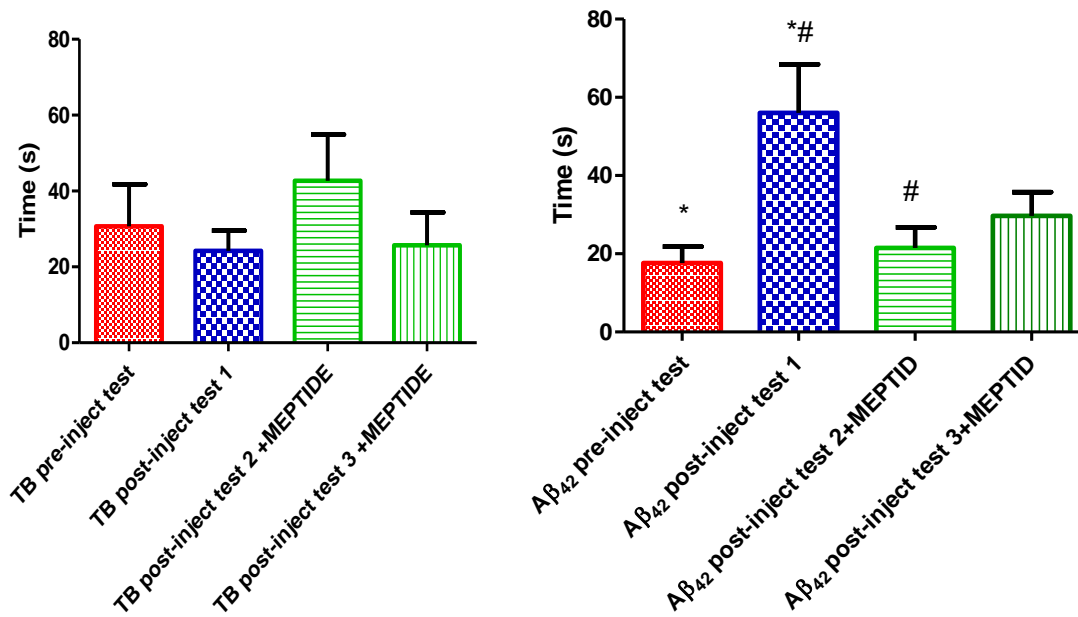


Figure 3.5: Graph showing time taken by MEPTIDES-treated TB-injected and A β_{42} -injected rats to find the hidden platform in the MWM. The significant difference observed between the pre-injection test vs the post-injection test 1, which is the first test before i.p. injection of MEPTIDES in the A β_{42} -injected group (17.60 ± 4.24 vs 56.00 ± 12.41 , $*p < 0.05$) shows a decrease in ability to recall the location of the platform in the rats injected with A β_{42} and is similar to that of the A β_{42} -injected group in Figure 3.1. This time however, was significantly reduced 24 hours after the first i.p. injection of MEPTIDES in the same A β_{42} -injected group (56.00 ± 12.41 vs 21.50 ± 5.27 , $^{\#}p < 0.05$).

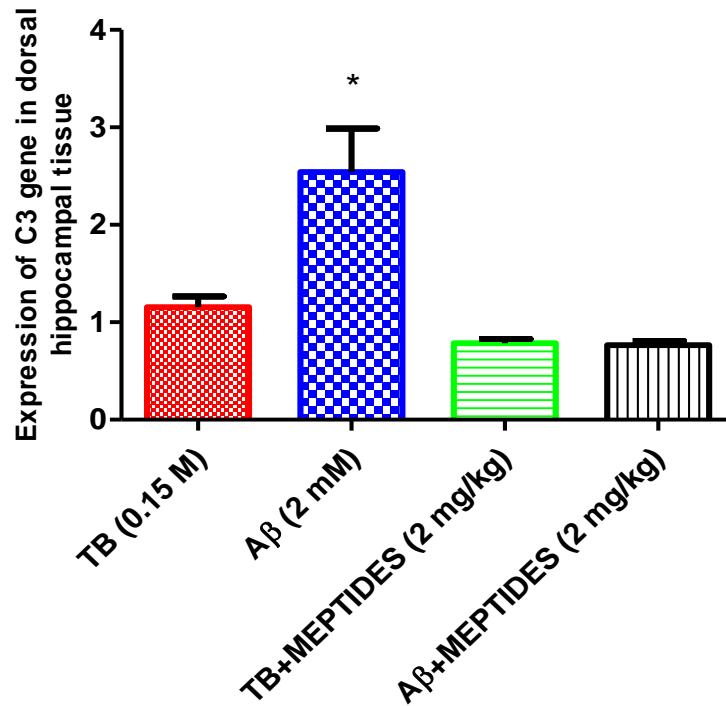
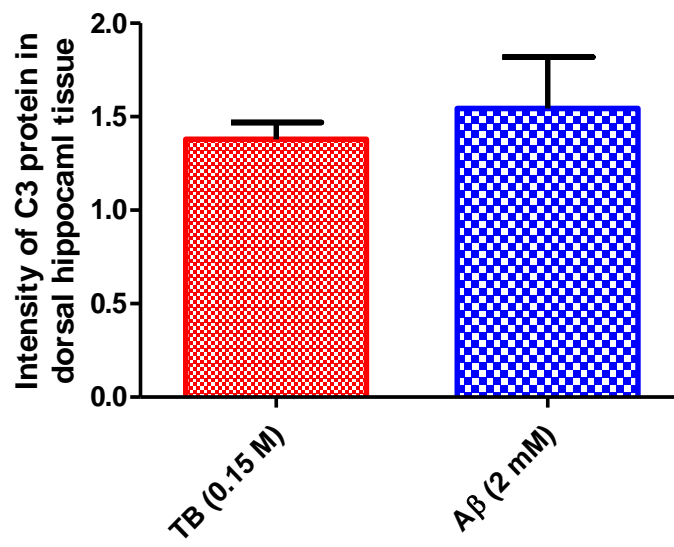
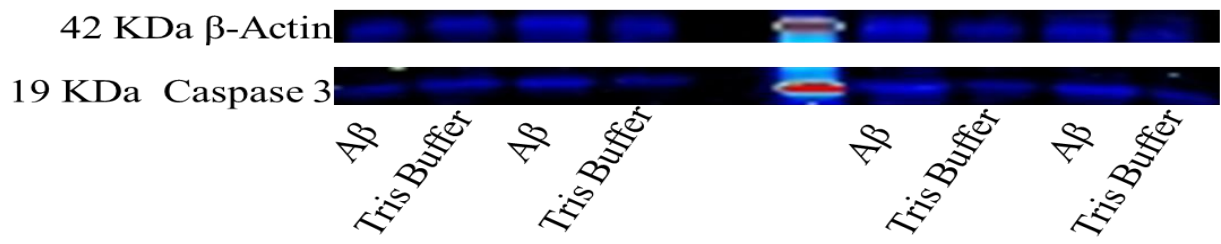


Figure 3.6: Graph showing qPCR expression of the C3 gene in the dorsal hippocampal tissue of TB- and A β_{42} -injected rats vs MEPTIDES (2 mg/kg)-treated TB- and A β_{42} -injected rats. The i.c A β_{42} injection significantly increased the expression of the C3 gene when the A β_{42} -injected rats were compared to TB-injected rats (2.54 ± 0.45 vs 1.16 ± 0.11 , * $p < 0.05$). Three injections of MEPTIDES (2 mg/kg, i.p.) over a 3-day period reversed the effect of A β_{42} on C3 gene expression when A β_{42} -injected rats were compared to the MEPTIDES-treated A β_{42} rats (2.54 ± 0.45 vs 0.77 ± 0.04 , * $p < 0.05$).

A



B

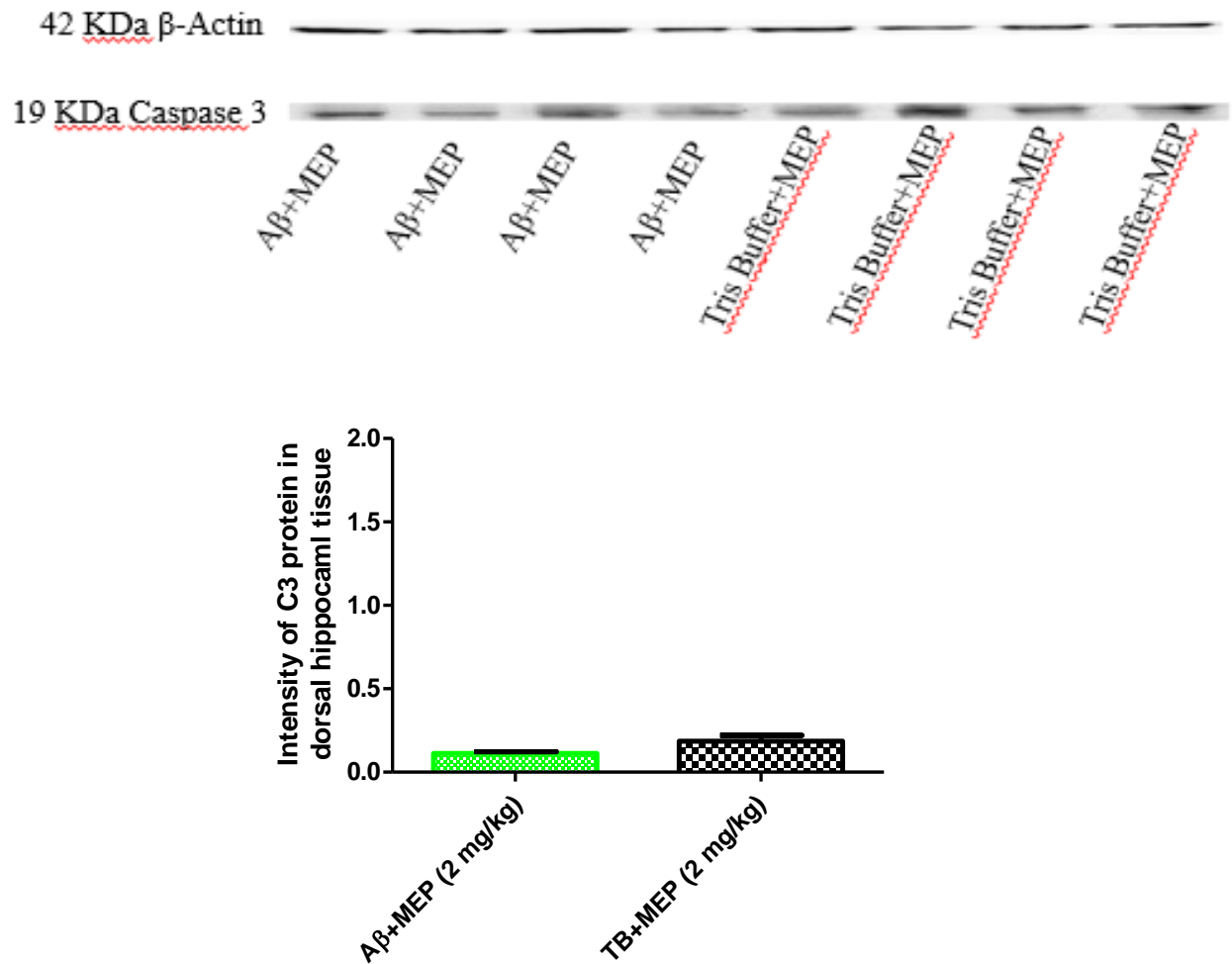
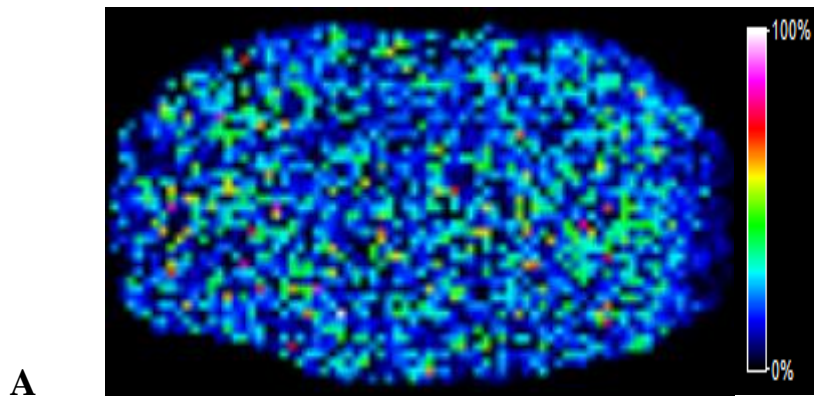
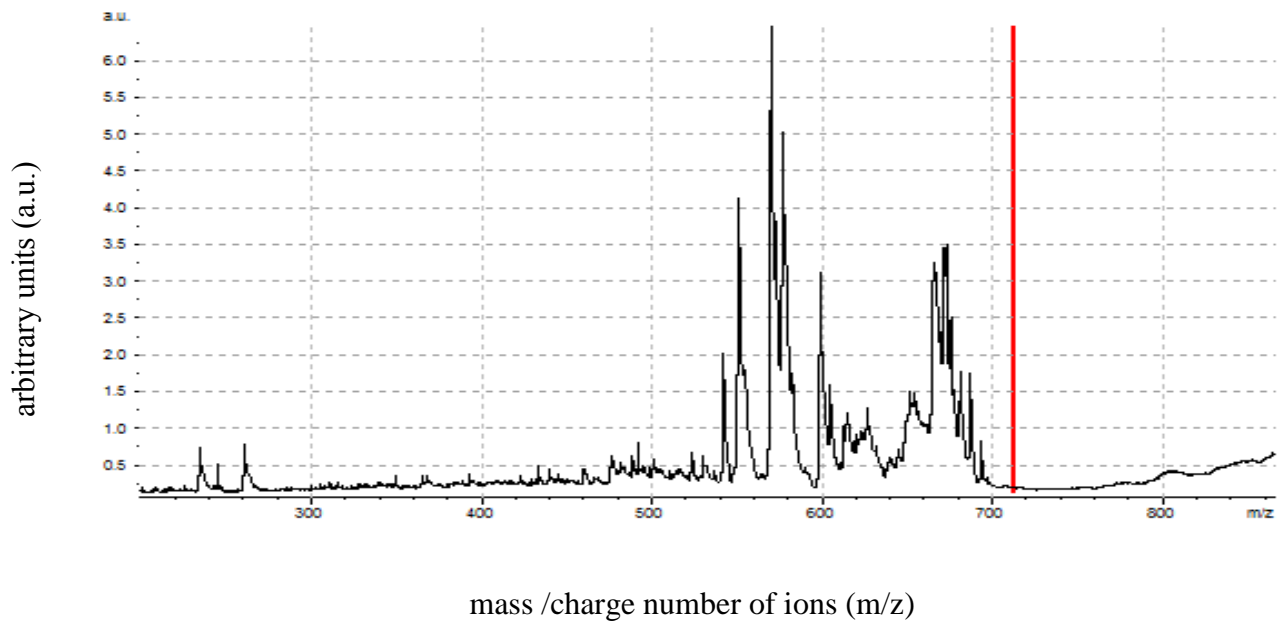
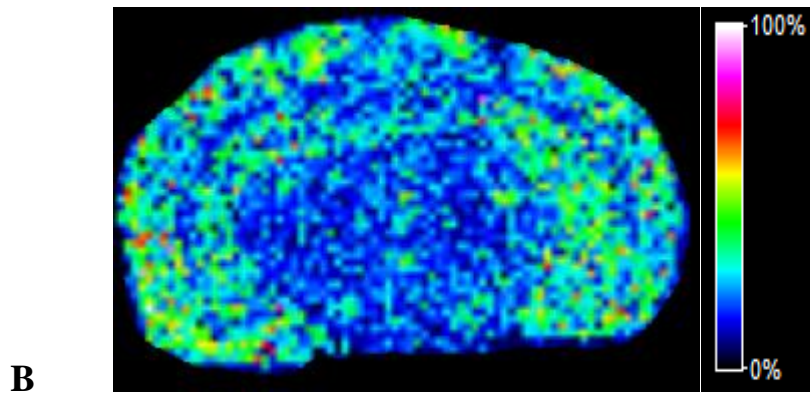


Figure 3.7: Graphs showing Western blot results for C3 protein levels in dorsal hippocampal tissue of TB-injected, A β -injected, and MEPTIDE (2 mg/kg)-treated rats. The t-test analysis of TB- vs A β -injected rats did not show any significant difference in dorsal hippocampal C3 levels (1.38 ± 0.09 vs 1.55 ± 0.27 , $p > 0.05$), (Figure 3.7 A). The t-test analysis of the MEPTIDE (2 mg/kg)-treated TB- vs A β -injected rats also did not show any significant difference when the 2 groups were compared (0.19 ± 0.04 vs 0.11 ± 0.01 , $p > 0.05$), (Figure 3.7 B).

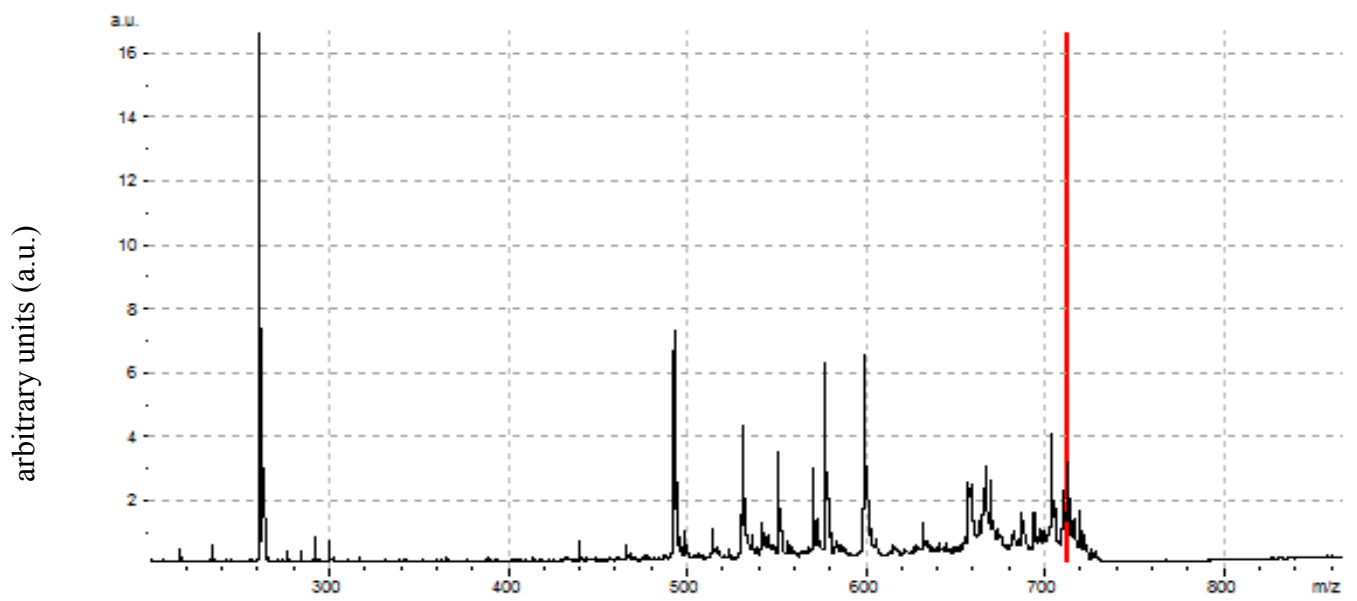


01: 712.413 Da \pm 0.2%





01: 712.413 Da \pm 0.2%



mass /charge number of ions (m/z)

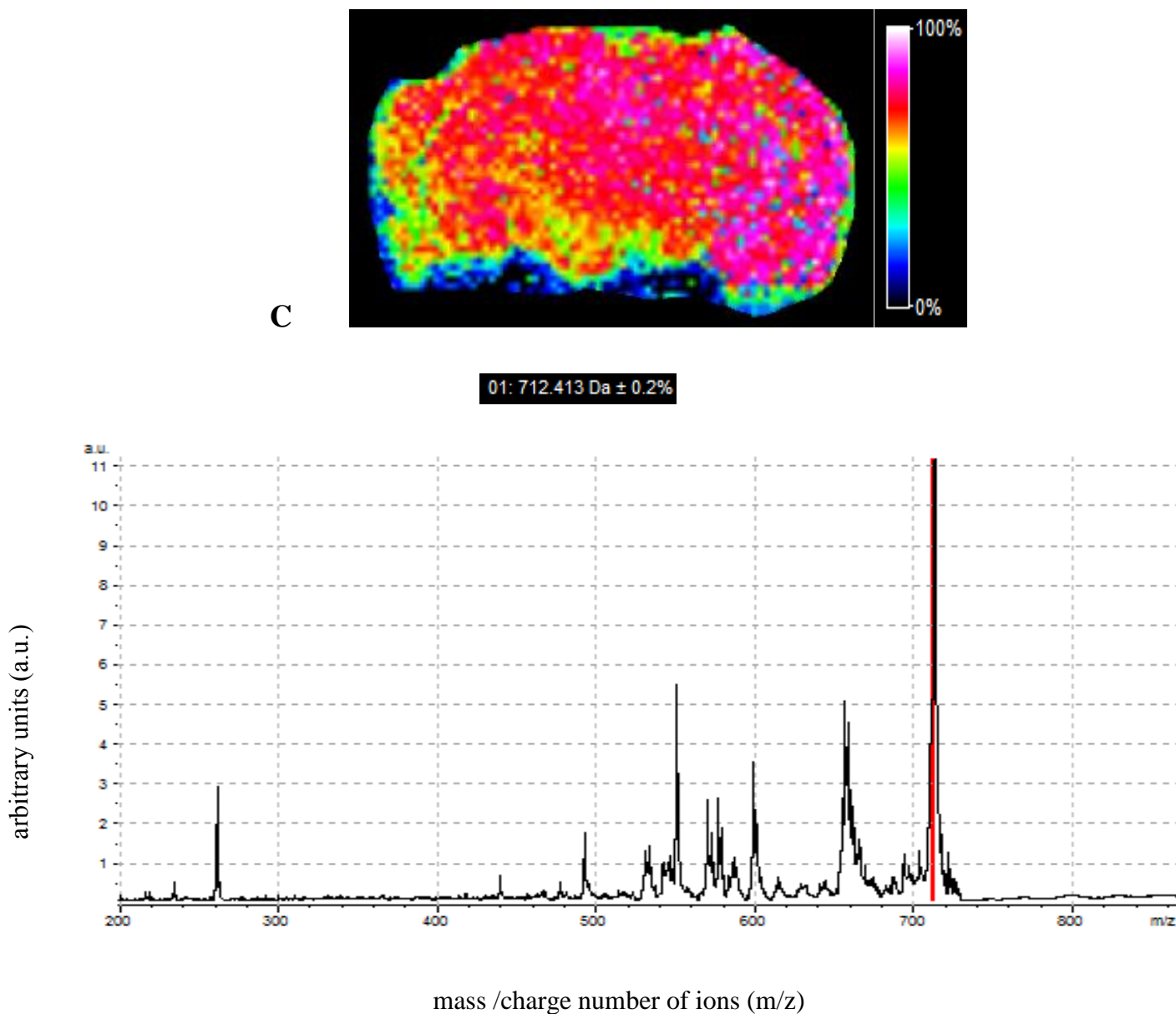


Figure 3.8: Diagrams showing presence and abundance of MEPTIDES derived metabolites in the rat brain. Figure 3.8 A shows naïve brain. Figure 3.8 B shows TB-injected MEPTIDES-treated rat brain. Figure 3.8 C shows $A\beta_{42}$ -injected MEPTIDES-treated rat brain. There was a higher abundance of the Na^+/K^+ adduct of the (690.04 ± 0.20 % and 674.13 ± 0.20 % m/z respectively) fragments in the MEPTIDES-treated $A\beta_{42}$ -injected brain (Figure 3.8 C) when it was compared to the MEPTIDES-treated TB-injected brain (712.41 ± 0.20 % m/z) (Figure 3.8 B). This peak was not observed in the control naïve brain (Figure 3.8 A). The peak of interest (712.41 ± 0.20 % m/z) in all MALDI TOF MS results is indicated by the red line. The colour legend represents the intensity of the peak of interest.

CHAPTER 4

Discussion

The hippocampus is one of the limbic structures of the brain that plays a prominent role in cognitive processes such as learning, memory storage and spatial navigation. Not surprisingly it is also the brain area that is first to show damage in people suffering from cognitive impairments (Colombo and Broadbent, 2000) . Because of its devastating effects on the quality of life, rodent models have been developed to study the pathophysiology of disorders associated with abnormalities in learning and memory.

The aims of the present study were to establish and characterize a rat model that may resemble some of the symptoms of AD and to evaluate the efficacy of MEPTIDES *in vivo* as a possible anti-AD drug.

In 2 studies we showed that a single i.c. injection of $A\beta_{42}$ into the dorsal hippocampus increased the time taken by rats to find the hidden platform in the MWM test. Rats treated with MEPTIDES for 3 days after the intra-hippocampal $A\beta_{42}$ injection found the platform in significantly less time than saline-treated rats, suggesting that the MEPTIDES had prevented the development of cognitive impairment in the $A\beta_{42}$ -injected rats. These findings are in agreement with previous studies where MEPTIDES were shown to reduce $A\beta_{42}$ -related neurotoxicity *in vitro* and in *Drosophila melanogaster*. Pratim Bose et al. (2009) Showed that di- or tri-methylation retarded the appearance of the β -structure of $A\beta_{40}$ to 4-5 hours and for $A\beta_{42}$ to 3 hours. Penta-methylation in contrast, completely prevented β -sheet formation by $A\beta_{40}$ during the time period studied and delayed the appearance of $A\beta_{42}$ β -sheet structure to 4 hours. This suggested that the penta-methylated peptide is more efficient than the less methylated peptides in reducing formation of oligomers with β -sheet structure from $A\beta_{40}$ and $A\beta_{42}$. The penta-methylated peptide resulted in prolonged life span in *Drosophila* expressing $A\beta_{42}$ but had no effect on the life span of wild type *Drosophila* treated with the penta-

methylated peptide only (Pratim Bose et al., 2009), indicating that the mode of action of MEPTIDES is A β specific. These results influenced and motivated the current investigations to evaluate whether MEPTIDES have similar effects in mammalian systems.

Behavioural results obtained in our study showed impairment in cognitive function of the A β_{42} -injected rats when they were compared to vehicle (TB) injected rats in the Morris Water Maze (MWM). The A β_{42} -injected rats took longer to find the hidden platform than vehicle-injected rats. Interestingly our findings show approximately 70 % of the A β_{42} -injected rats had difficulty completing the behavioural task during post-injection test 1, which is the test conducted 48 hours after the i.c. injection of A β_{42} . We attributed this observation to the toxic activity of our A β_{42} . These findings were significant in the context that 60 % of AD patients do not display cognitive deficit symptoms until the disease reaches severe stages (Findeis, 2007). Our data confirmed the damaging effects of A β_{42} , and highlights the devastating consequences it may have when left uncontrolled. However, we also recognize that AD is progressive in nature, and develops over many years. We therefore proposed that learning and memory deficits may not be the earliest sign of AD and that there may be other earlier markers of this detrimental disease.

It is undoubtable that there is increased inflammation in the AD brain, and microglia contribute largely to this inflammation (Frautschy et al., 1998). The neuro-inflammatory response is therefore thought to be a secondary event subsequent to neuronal damage and degeneration. Inflammation in AD can be described as an upregulation of the inflammatory pathway that initially acts as a defense mechanism in response to increased A β aggregation/plaque formation in the brain (Simic et al., 2009). Strangely some cytokines including TNF- α , have been observed to increase plaque formation by altering APP processing via upregulation of the β -secretase enzyme (Heneka and O'Banion, 2007), the rate-limiting enzyme in A β production (Cole and Vassar, 2007). This observation has been supported by studies indicating that the majority of the neurotoxic effects attributed to microglia are exerted by TNF- α in the AD brain (Heneka and O'Banion, 2007). It has subsequently been speculated that TNF- α contributes to A β formation by causing sustained activation of the β -secretase pathway leading to A β production in a vicious cycle that ultimately causes cell death. In contrast TNF- α (Rogers et al., 1996) suggested to protect

against glutamate, ROS and A β neurotoxicity (Akiyama et al., 2000) in AD. The function of TNF- α may be concentration dependent as previous findings by Johnstone et al. (1999) which showed that A β_{40} and A β_{42} stimulated the release of chemokines and TNF- α in particular, to different extents. In our experiments we measured TNF- α using a sandwich ELISA and found no differences between control and A β_{42} rats. While our data appear to be contrary to those of others, the difference in findings may be a result of variations in experimental protocols.

Increased production of ROS/free radicals leads to oxidative stress (Rosenfeldt et al., 2013) and ultimately apoptosis (Loo et al., 1993). Detection of these pathophysiological entities has been proposed as possible early biomarkers of AD. 4HNE is a major cytotoxic product from the class of α - and β -unsaturated aldehydes (Camandola et al., 2000) that is used as a marker for the occurrence and extent of lipid peroxidation (Schneider et al., 2001). We found that A β_{42} injection into the dorsal hippocampus did not alter 4HNE levels when compared to vehicle-injected control rats. The results of the present study therefore suggest that A β_{42} injection into the dorsal hippocampus does not increase lipid peroxidation or oxidative stress in the rat brain. A study by Tsurunikov et al. (2012) demonstrated that the deacetylation of mercapturic acids formed in the GSH conjugation metabolism of 4HNE is aminoacylase 3 (AA3) mediated in neurons and might initiate a chain of reactions leading to transformation of macromolecules that might participate in AD pathology. Although data from our study is in contrast to earlier studies reporting elevated levels of HNE-lysine adducts in AD hippocampal tissue sections and increased 4HNE levels in N2a/D9 cells (Sayre et al., 1997, Liu et al., 2013), it is supported by a study by Yao et al. (1999) which showed that lipid peroxidation does not mediate A β -induced cell death in PC 12 cells, and we postulate that this may in part responsible for the results of the present study. We cannot neglect vast differences in results associated with studies conducted *in vitro* and *in vivo*. We also believe that our experimental timeline for the animal studies was short for detectable differences in the 4HNE levels, as this marker is used to measure chronic oxidative stress.

Caspases are a family of aspartate-specific cysteinyl proteases that are produced as catalytically inactive zymogens in cells (Chai et al., 2000). Executioner caspases-3 and -7 are a subset that cleaves specific substrates leading to alterations linked to apoptosis viz. chromatin condensation, DNA fragmentation, blebbing of plasma membrane, cell shrinkage

and ultimately cell death (Kasibhatla and Tseng, 2003). A biochemical feature associated with apoptosis is the expression of cell surface markers. The externalisation of phosphatidylserine (PS), a transmembrane glycoprotein of the phospholipid bilayer signals early phagocytosis of apoptotic cells with minimal compromise to adjacent and surrounding tissue (Bratton et al., 1997). Mitochondria play an important role in apoptosis, via the intrinsic apoptotic program. An initial crucial step for activation of the intrinsic apoptotic pathway is depolarisation of the mitochondrial membrane. Depolarised mitochondrial membranes occur as a result of the formation of mitochondrial permeability transition (PT) pores (Hirsch et al., 1997). Altered mitochondrial PT has been associated with various metabolic consequences such as halted functioning of the electron transport chain (ETC) with associated elevation in ROS and decreased production of cellular ATP (Wang, 2001). Bax, a pro-apoptotic protein of the Bcl-2 family, translocates from the cytosol to the outer mitochondrial membrane during apoptosis where it interacts with lipids and induces mitochondrial PT pores. Findings from Loo et al. (1993) showed severe surface blebbing, internucleosomal DNA fragmentation and shrunken neurons in cultured neurons 24 hours after exposure to A β . In another study by Awasthi et al. (2005), A β ₄₂ inhibited cell proliferation by approximately 80 % when compared to the control value, caused morphological changes to the cells in a dose- and time-dependent manner and caused apoptosis of IMR-32 cells through activation of caspase-8, -9 and -3. It was concluded in this study that A β ₄₂ activated initiator caspase-9, which is responsible for the activation of executioner C3 which causes apoptosis. In our study we observed an upregulation of the C3 gene but no change C3 protein levels as a result of A β ₄₂ injection into the dorsal hippocampus compared to control vehicle-injected rats, using qPCR and Western blot. This is an interesting finding as it indicates increased gene transcription, without concomitant raise in protein level. A reasonable explanation for this observation may be that C3 turnover could have been accelerated. However the catabolic products of C3 have not been measured in the present study, so this explanation remains speculative. Nevertheless misalignment between gene transcription and protein synthesis is not new, since other researchers have experienced similar results. A study by Glanemann et al. (2003) showed that large increases in gene expression are not congruent with changes in enzyme activity. In another study, Ghazalpour et al. (2011) showed that levels of transcripts and proteins correlated significantly for only about 50 % of the genes that they tested, with an average correlation of 0.27, and these correlations varied depending on the cellular location and biological function of the gene. Schwanhausser et al. (2011) Found that mRNA levels only explained around 40% of the variability in protein

levels, and protein abundance seemed to be predominantly regulated at the ribosome, which highlighted the importance of translational control. Compared to translational control, protein stability seems to have a minor role in cellular protein abundance. Despite the vast literature available on misalignment between gene transcription and protein synthesis, we speculate that on such a closely regulated cascade like the C3 apoptotic cascade, it necessary to gain insight into the exact time point of the synthesis C3 protein in the pathway to be able to detect any subtle changes in its expression thereof. We postulate that C3 protein may not have a direct impact in behavior from the present study; it is rather the changes in the abundance and distribution of the C3 and other proteins which are responsible for the behavioural changes that we observed.

Promising, was the fact that MEPTIDES showed positive effects on behaviour and also down-regulated C3 gene expression increases induced by A β ₄₂. Pratim Bose et al. (2009) Found that MEPTIDES could be incorporated into the hydrophobic core of A β oligomers and thus prevent A β aggregation *in vitro*. This was proposed as the mechanism of action of MEPTIDES in lowering A β associated toxicity *in vitro*. Another study by Awasthi et al. (2005) where short peptide A β ₁₅₋₂₂, (8 AAs in length) were used, reported an inhibition of A β ₄₂ self-aggregation and hydrolytic activities *in vivo*. This decrease was accompanied by a corresponding decrease in A β -induced apoptosis. In a similar study by Sigurdsson et al. (2000), pentapeptides LPFFD suggested *in vivo* reversal of A β lesion in the rat brain. We postulate that the mechanism of action of MEPTIDES *in vivo* may be the same as its action *in vitro* and similar to what other previously reported short peptides of variable lengths of A β have shown. But it is not known whether MEPTIDES cross the blood brain barrier, and since methylation changes the chemical properties and confers rigidity to a compound which may affect its behaviour in several environments, it became necessary that we determined whether MEPTIDES did in fact cross the blood brain barrier in order to be able to attribute the effects that we have observed solely to the MEPTIDES. This was performed by MALDI-TOF MS.

The MALDI-TOF results revealed that there was a significantly greater abundance of the Na⁺/K⁺ adduct (\approx 713Da) of the fragments that were previously obtained during the optimization process in the A β ₄₂ + MEPTIDES brain when it was compared to TB + MEPTIDES brain. We did not observe this peak in the control naïve brain. Silverberg et al.

(2003) Found that there was a coexistence of AD and adult-onset normal pressure chronic hydrocephalus (NPH) suggesting that AD and NPH are related and have a common physiological basis in cerebrospinal fluid (CSF) circulatory dysfunction and failure. CSF functions include buoyancy, acid base buffering and transport of molecules and micronutrients to and from the brain parenchyma. Failure of CSF to detoxify the brain may lead to aggregation of A β and other unidentified toxins (Silverberg et al., 2003). Endothelial receptors for A β disappear with age, this leads to increased parenchymal A β deposition since A β has been observed to cross the BBB via capillaries and this happens to also be the primary route for its clearance (Silverberg et al., 2003). However, A β overproduction is not the only factor that determines whether A β will aggregate or not, particularly in late onset AD where A β overproduction does not seem to play a role (DeMattos et al., 2002). Other factors controlling local metabolism as well as clearance to plasma also seem to play a role (DeMattos et al., 2002). We postulate that it is these disruptions in CSF chemistry and BBB membrane integrity coupled with the A β specific nature of MEPTIDES (Pratim Bose et al., 2009) that lead to greater penetrance of MEPTIDES into the A β_{42} -exposed brain where it is able to perform the function of lowering A β_{42} associated neurotoxicity.

CHAPTER 5

Summary and Conclusion

5.0 Summary

Substantial evidence exists that indicate $A\beta$ to be one of the etiological factors in the development of AD. Since memory impairment is central to this neurological disorder, the present study focused on this characteristic symptom to investigate the possible therapeutic potential of a novel drug. The aims of the present study were to, establish and characterize a rat model that mimics the cognitive symptoms of AD and to evaluate the efficacy of MEPTIDES *in vivo* as a possible anti-AD drug. A single i.c. injection of $A\beta_{42}$ (2 mM) was administered stereotaxically into the dorsal hippocampus of adult male SD rats and spatial learning and memory tests were conducted using the MWM. The rats showed deficits in learning and memory following intra-hippocampal injection of $A\beta_{42}$, and these deficits were reversed by i.p. injections of MEPTIDES (2 mg/kg) over a 3 day period. Biochemical analysis of hippocampal brain tissue showed upregulation of the C3 gene in the $A\beta_{42}$ rats. There was a downregulation of the C3 gene but no difference in C3 protein levels in the $A\beta_{42}$ rats that also received MEPTIDES i.p. There was also a high abundance of Na^+/K^+ adducts of the MEPTIDES fragments in the $A\beta_{42}$ -injected brain when compared to the vehicle-injected rat brain. The present study is the first study to document that MEPTIDES cross BBB and it is also the first study to document the *in vivo* effects of MEPTIDES.

5.1 Conclusion

Findings from this study showed that a single bilateral intrahippocampal injection of $A\beta_{42}$ induces deficits in cognitive function in adult male SD rats by upregulating the C3 driven apoptotic pathway. MEPTIDES administered intraperitoneally get into the brain parenchyma in order to attenuate $A\beta_{42}$ induced behavioural deficits. The mechanisms, by which MEPTIDES do so, include the downregulation of the C3 cascade. Our study further suggests that C3 cascade disruptions may be amongst the earliest markers of $A\beta_{42}$ -induced neurotoxicity.

REFERENCES

- AKIYAMA, H., BARGER, S., BARNUM, S., BRADT, B., BAUER, J., COLE, G. M., COOPER, N. R., EIKELENBOOM, P., EMMERLING, M., FIEBICH, B. L., FINCH, C. E., FRAUTSCHY, S., GRIFFIN, W. S. T., HAMPEL, H., HULL, M., LANDRETH, G., LUE, L. F., MRAK, R., MACKENZIE, I. R., MCGEER, P. L., O'BANION, M. K., PACHTER, J., PASINETTI, G., PLATA-SALAMAN, C., ROGERS, J., RYDEL, R., SHEN, Y., STREIT, W., STROHMEYER, R., TOOYOMA, I., VAN MUISWINKEL, F. L., VEERHUIS, R., WALKER, D., WEBSTER, S., WEGRZYNIAK, B., WENK, G. & WYSS-CORAY, T. 2000. Inflammation and Alzheimer's disease. *Neurobiology of Aging*, 21, 383-421.
- AWASTHI, A., MATSUNAGA, Y. & YAMADA, T. 2005. Amyloid-beta causes apoptosis of neuronal cells via caspase cascade, which can be prevented by amyloid-beta-derived short peptides. *Experimental Neurology*, 196, 282-289.
- BARMAN, A. & PRABHAKAR, R. 2013. Elucidating the catalytic mechanism of β -secretase (BACE1): A quantum mechanics/molecular mechanics (QM/MM) approach. *Journal of Molecular Graphics and Modelling*, 40, 1-9.
- BAYER, T. A. & WIRTHS, O. 2010. Intracellular accumulation of amyloid-Beta - a predictor for synaptic dysfunction and neuron loss in Alzheimer's disease. *Frontiers in Aging Neuroscience*, 2, 8.
- BEHL, C. & MOOSMANN, B. 2002. Antioxidant neuroprotection in Alzheimer's disease as preventive and therapeutic approach. *Free Radical Biology and Medicine*, 33, 182-191.
- BOSE, P. P., CHATTERJEE, U., NERELIUS, C., GOVENDER, T., NORSTROM, T., GOGOLL, A., SANDEGREN, A., GOTHELID, E., JOHANSSON, J. & ARVIDSSON, P. I. 2009. Poly N-methylated Amyloid Beta- Peptide C- Terminal Fragments Reduce Amyloid Beta Toxicity in Vitro and in Drosophila melanogaster. *Medicinal Chemistry*, 52, 8002-8009.
- BRATTON, D. L., FADOK, V. A., RICHTER, D. A., KAILEY, J. M., GUTHRIE, L. A. & HENSON, P. M. 1997. Appearance of phosphatidylserine on apoptotic cells requires calcium-mediated nonspecific flip-flop and is enhanced by loss of the aminophospholipid translocase. *J Biol Chem*, 272, 26159-65.

- CAMANDOLA, S., POLI, G. & MATTSON, M. P. 2000. The lipid peroxidation product 4-hydroxy-2, 3-nonenal increases AP-1-binding activity through caspase activation in neurons. *Journal of Neurochemistry*, 74, 159-168.
- CAMERON, B. & LANDRETH, G. E. 2010. Inflammation, microglia, and alzheimer's disease. *Neurobiology of Disease*, 37, 503-509.
- CETIN, F. 2013. *Role of Oxidative Stress in A β Animal Model of Alzheimer's Disease: Vicious Circle of Apoptosis, Nitric Oxide and Age*.
- CHAI, J., DU, C., WU, J. W., KYIN, S., WANG, X. & SHI, Y. 2000. Structural and biochemical basis of apoptotic activation by Smac/DIABLO. *Nature*, 406, 855-62.
- CHU, L. 2012. Alzheimer's disease: early diagnosis and treatment. *Hong Kong Med J*, 18, 228-237.
- COLE, S. & VASSAR, R. 2007. The Alzheimer's disease beta-secretase enzyme, BACE1. *Molecular Neurodegeneration*, 2, 22.
- COLOMBO, M. & BROADBENT, N. 2000. Is the avian hippocampus a functional homologue of the mammalian hippocampus? *Neuroscience & Biobehavioral Reviews*, 24, 465-484.
- CREWS, L., ROCKENSTEIN, E. & MASLIAH, E. 2010. APP transgenic modeling of Alzheimer's disease: mechanisms of neurodegeneration and aberrant neurogenesis. *Brain Structure and Function*, 214, 111-126.
- DEGUIL, J., RAVASI, L., AUFFRET, A., BABILONI, C., BARTRES FAZ, D., BRAGULAT, V., CASSÉ-PERROT, C., COLAVITO, V., HERRERO EZQUERRO, M. T., LAMBERTY, Y., LANTEAUME, L., PEMBERTON, D., PIFFERI, F., RICHARDSON, J. C., SCHENKER, E., BLIN, O., TARRAGON, E. & BORDET, R. 2013. Evaluation of symptomatic drug effects in Alzheimer's disease: strategies for prediction of efficacy in humans. *Drug Discovery Today: Technologies*, 10, e329-e342.
- DELRIEU, J., OUSSET, P. J., CAILLAUD, C. & VELLAS, B. 2012. 'Clinical trials in Alzheimer's disease': immunotherapy approaches. *Journal of Neurochemistry*, 120, 186-193.
- DEMATOS, R. B., BALES, K. R., PARSADANIAN, M., O'DELL, M. A., FOSS, E. M., PAUL, S. M. & HOLTZMAN, D. M. 2002. Plaque-associated disruption of CSF and plasma amyloid-beta (A β) equilibrium in a mouse model of Alzheimer's disease. *J Neurochem*, 81, 229-36.

- EIKELENBOOM, P. & VAN GOOL, W. A. 2004. Neuroinflammatory perspectives on the two faces of Alzheimer's disease. *Journal of Neural Transmission*, 111, 281-294.
- FARLOW, M. R., SALLOWAY, S., TARIOT, P. N., YARDLEY, J., MOLINE, M. L., WANG, Q., BRAND-SCHIEBER, E., ZOU, H., HSU, T. & SATLIN, A. 2010. Effectiveness and tolerability of high-dose (23 mg/d) versus standard-dose (10 mg/d) donepezil in moderate to severe alzheimer's disease: a 24-week, randomized, double-blind study. *Clinical therapeutics*, 32, 1234-1251.
- FEN, L., XU, L., AI-QIN, S. & JIE-WEN, Z. 2010. Inhibition of tau hyperphosphorylation and Beta Amyloid production in rat brain by oral administration of atorvastatin. *Chinese Medical Journal*, 123, 1864-1870.
- FINDEIS, M. A. 2007. The role of amyloid [beta] peptide 42 in Alzheimer's disease. *Pharmacology & Therapeutics*, 116, 266-286.
- FRAUTSCHY, S. A., YANG, F., IRRIZARRY, M., HYMAN, B., SAIDO, T. C., HSIAO, K. & COLE, G. M. 1998. Microglial response to amyloid plaques in APPsw transgenic mice. *Am J Pathol*, 152, 307-17.
- FREIR, D. B., COSTELLO, D. A. & HERRON, C. E. 2003. A β 25–35-Induced Depression of Long-Term Potentiation in Area CA1 In Vivo and In Vitro Is Attenuated by Verapamil. *Journal of Neurophysiology*, 89, 3061-3069.
- FUNKE, S. A. & WILLBOLD, D. 2012. Peptides for Therapy and Diagnosis of Alzheimer's Disease. *Current Pharmaceutical Design*, 18, 755-767.
- GHAZALPOUR, A., BENNETT, B., PETYUK, V. A., OROZCO, L., HAGOPIAN, R., MUNGRUE, I. N., FARBER, C. R., SINSHEIMER, J., KANG, H. M., FURLOTTE, N., PARK, C. C., WEN, P. Z., BREWER, H., WEITZ, K., CAMP, D. G., 2ND, PAN, C., YORDANOVA, R., NEUHAUS, I., TILFORD, C., SIEMERS, N., GARGALOVIC, P., ESKIN, E., KIRCHGESSNER, T., SMITH, D. J., SMITH, R. D. & LUSIS, A. J. 2011. Comparative analysis of proteome and transcriptome variation in mouse. *PLoS Genet*, 7, e1001393.
- GIBSON, G. E. 2002. Interactions of oxidative stress with cellular calcium dynamics and glucose metabolism in Alzheimer's disease. *Free Radical Biology and Medicine*, 32, 1061-1070.
- GLANEMANN, C., LOOS, A., GORRET, N., WILLIS, L. B., O'BRIEN, X. M., LESSARD, P. A. & SINSKEY, A. J. 2003. Disparity between changes in mRNA abundance and enzyme activity in *Corynebacterium glutamicum*: implications for DNA microarray analysis. *Applied Microbiological Biotechnology*, 61, 61-8.

- HALL, A. M. & ROBERSON, E. D. 2012. Mouse models of Alzheimer's disease. *Brain Research Bulletin*, 88, 3-12.
- HENEKA, M. T. & O'BANION, M. K. 2007. Inflammatory processes in Alzheimer's disease. *Journal of Neuroimmunology*, 184, 69-91.
- HETÉNYI, C., SZABÓ, Z., KLEMENT, É., DATKI, Z., KÖRTVÉLYESI, T., ZARÁNDI, M. & PENKE, B. 2002. Pentapeptide Amides Interfere with the Aggregation of β -Amyloid Peptide of Alzheimer's Disease. *Biochemical and Biophysical Research Communications*, 292, 931-936.
- HIRSCH, T., MARCHETTI, P., SUSIN, S. A., DALLAPORTA, B., ZAMZAMI, N., MARZO, I., GEUSKENS, M. & KROEMER, G. 1997. The apoptosis-necrosis paradox. Apoptogenic proteases activated after mitochondrial permeability transition determine the mode of cell death. *Oncogene*, 15, 1573-81.
- HUANG, H. J., LIANG, K. C., CHEN, C. P., CHEN, C. M. & HSIEH-LI, H. M. 2007. Intrahippocampal administration of Amyloid Beta(1-40) impairs spatial an learning memory in hyperglycemic mice. *Neurobiology of Learning and Memory*, 87, 483-494.
- IRIE, K., MURAKAMI, K., MASUDA, Y., MORIMOTO, A., OHIGASHI, H., OHASHI, R., TAKEGOSHI, K., NAGAO, M., SHIMIZU, T. & SHIRASAWA, T. 2005. Structure of Beta-Amyloid fibrils and its relevance to their neurotoxicity: Implications for the pathogenesis of Alzheimer's disease. *Journal of Bioscience and Bioengineering*, 99, 437-447.
- JOHNSTONE, M., GEARING, A. J. H. & MILLER, K. M. 1999. A central role for astrocytes in the inflammatory response to β -amyloid; chemokines, cytokines and reactive oxygen species are produced. *Journal of Neuroimmunology*, 93, 182-193.
- KASIBHATLA, S. & TSENG, B. 2003. Why Target Apoptosis in Cancer Treatment? *Molecular Cancer Therapeutics*, 2, 573-580.
- KRUGER, N. 2009. The Bradford Method For Protein Quantitation. *In: WALKER, J. (ed.) The Protein Protocols Handbook*. Humana Press.
- KUMAR, P., TAHA, A., KALE, R. K., COWSIK, S. M. & BAQUER, N. Z. 2011. Physiological and biochemical effects of 17[beta] estradiol in aging female rat brain. *Experimental Gerontology*, 46, 597-605.
- LEE, J., GIORDANO, S. & ZHANG, J. 2012. Autophagy, mitochondria and oxidative stress: cross-talk and redox signalling. *Biochemical Journal*, 441, 523-540.

- LIU, J., CHI, N., CHEN, H., ZHANG, J., BIAN, Y., CUI, G. & XIU, C. 2013. Resistin protection against endogenous A β neuronal cytotoxicity from mitochondrial pathway. *Brain Research*, 1523, 77-84.
- LOO, D. T., COPANI, A., PIKE, C. J., WHITTEMORE, E. R., WALENCEWICZ, A. J. & COTMAN, C. W. 1993. Apoptosis is induced by beta-amyloid in cultured central nervous system neurons. *Proceedings of the National Academy of Sciences*, 90, 7951-7955.
- MACKRAJ, I., RAMESAR, S., SINGH, M., GOVENDER, T., BAIJNATH, H., SINGH, R. & GATHIRAM, P. 2008. The in vivo effects of *Tulbhagia violacea* on blood pressure in a salt-sensitive rat model. *Journal of Ethnopharmacology*, 117, 263-269.
- MADSEN, S. K., HO, A. J., HUA, X., SAHARAN, P. S., TOGA, A. W., JACK JR, C. R., WEINER, M. W. & THOMPSON, P. M. 2010. 3D maps localize caudate nucleus atrophy in 400 Alzheimer's disease, mild cognitive impairment, and healthy elderly subjects. *Neurobiology of Aging*, 31, 1312-1325.
- MAMELAK, M. 2007. Alzheimer's disease, oxidative stress and gammahydroxybutyrate. *Neurobiology of Aging*, 28, 1340-1360.
- MANDEL, S., AMIT, T., BAR-AM, O. & YODIM, M. B. H. 2007. Iron dysregulation in Alzheimer's disease: Multimodal brain permeable iron chelating drugs, possessing neuroprotective-neurorescue and amyloid precursor protein-processing regulatory activities as therapeutic agents. *Progress in Neurobiology*, 82, 348-360.
- MANDELL, A. M. & GREEN, R. C. 2011. *Alzheimer's disease*, Blackwell Publishing Ltd.
- MATHEW, A., YOSHIDA, Y., MAEKAWA, T. & SAKTHI KUMAR, D. 2011. Alzheimer's disease: Cholesterol a menace? *Brain Research Bulletin*, 86, 1-12.
- MCCUSKER, S. M., CURRAN, M. D., DYNAN, K. B., MCCULLAGH, C. D., URQUHART, D. D., MIDDLETON, D., PATTERSON, C. C., MCILROY, S. P. & PETER PASSMORE, A. 2001. Association between polymorphism in regulatory region of gene encoding tumour necrosis factor α and risk of Alzheimer's disease and vascular dementia: a case-control study. *The Lancet*, 357, 436-439.
- MORGAN, D. 2006. Immunotherapy for Alzheimer's disease. *Journal of Alzheimer's Disease* 9, 425-32.
- NICOLL, J. A., MRAK, R. E., GRAHAM, D. I., STEWART, J., WILCOCK, G., MACGOWAN, S., ESIRI, M. M., MURRAY, L. S., DEWAR, D. & LOVE, S. 2000. Association of interleukin-1 gene polymorphisms with Alzheimer's disease. *Annals of neurology*, 47, 365.

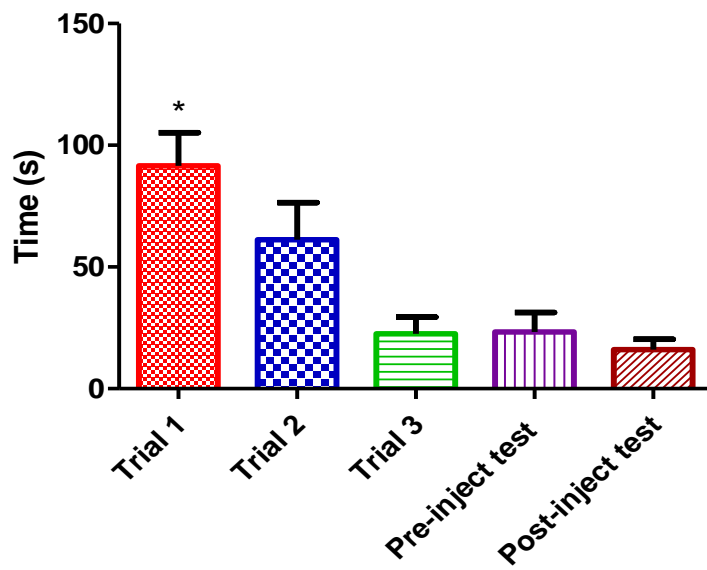
- PAPASSOTIROPOULOS, A., BAGLI, M., JESSEN, F., BAYER, T. A., MAIER, W., RAO, M. L. & HEUN, R. 1999. A genetic variation of the inflammatory cytokine interleukin-6 delays the initial onset and reduces the risk for sporadic Alzheimer's disease. *Annals of neurology*, 45, 666-668.
- PERRY, G., CASH, A. D. & SMITH, M. A. 2002. Alzheimer Disease and Oxidative Stress. *Journal of Biomedicine and Biotechnology*, 2, 120-123.
- PRATIM BOSE, P., CHATTERJEE, U., NERELIUS, C., GOVENDER, T., NORSTRÖM, T., GOGOLL, A., SANDEGREN, A., GÖTHELID, E., JOHANSSON, J. & ARVIDSSON, P. I. 2009. Poly-N-methylated Amyloid β -Peptide ($A\beta$) C-Terminal Fragments Reduce $A\beta$ Toxicity in Vitro and in *Drosophila melanogaster*. *Journal of Medicinal Chemistry*, 52, 8002-8009.
- REDDY, P. H. 2011. Abnormal tau, mitochondrial dysfunction, impaired axonal transport of mitochondria, and synaptic deprivation in Alzheimer's disease. *Brain Research*, 1415, 136-148.
- ROGERS, J., WEBSTER, S., LUE, L.-F., BRACHOVA, L., HAROLD CIVIN, W., EMMERLING, M., SHIVERS, B., WALKER, D. & MCGEER, P. 1996. Inflammation and Alzheimer's disease pathogenesis. *Neurobiology of Aging*, 17, 681-686.
- ROMANI, B., ENGELBRECHT, S. & GLASHOFF, R. H. 2010. Functions of Tat: the versatile protein of human immunodeficiency virus type 1. *Journal of General Virology*, 91, 1-12.
- ROSENFELDT, F., WILSON, M., LEE, G., KURE, C., OU, R., BRAUN, L. & DE HAAN, J. 2013. Oxidative stress in surgery in an ageing population: Pathophysiology and therapy. *Experimental Gerontology*, 48, 45-54.
- SAYRE, L. M., ZELASKO, D. A., HARRIS, P. L. R., PERRY, G., SALOMON, R. G. & SMITH, M. A. 1997. 4-Hydroxynonenal-Derived Advanced Lipid Peroxidation End Products Are Increased in Alzheimer's Disease. *Journal of Neurochemistry*, 68, 2092-2097.
- SCHNEIDER, C., TALLMAN, K. A., PORTER, N. A. & BRASH, A. R. 2001. Two distinct pathways of formation of 4-hydroxynonenal. Mechanisms of nonenzymatic transformation of the 9- and 13-hydroperoxides of linoleic acid to 4-hydroxyalkenals. *J Biol Chem*, 276, 20831-8.

- SCHWANHAUSSER, B., BUSSE, D., LI, N., DITTMAR, G., SCHUCHHARDT, J., WOLF, J., CHEN, W. & SELBACH, M. 2011. Global quantification of mammalian gene expression control. *Nature*, 473, 337-42.
- SHIN, R. W., OGINO, K., KONDO, A., SAIDO, T. C., TROJANOWSKI, J. Q., KITAMOTO, T. & TATEISHI, J. 1997. Amyloid beta-protein (Abeta) 1-40 but not Abeta1-42 contributes to the experimental formation of Alzheimer disease amyloid fibrils in rat brain. *Journal of Neuroscience*, 17, 8187-93.
- SIGURDSSON, E. M., PERMANNE, B., SOTO, C., WISNIEWSKI, T. & FRANGIONE, B. 2000. In vivo reversal of amyloid-beta lesions in rat brain. *J Neuropathol Exp Neurol*, 59, 11-7.
- SILVERBERG, G. D., MAYO, M., SAUL, T., RUBENSTEIN, E. & MCGUIRE, D. 2003. Alzheimer's disease, normal-pressure hydrocephalus, and senescent changes in CSF circulatory physiology: a hypothesis. *The Lancet Neurology*, 2, 506-511.
- SIMIC, G., STANIĆ, G., MLADINOV, M., JOVANOVIĆ-MILOSEVIC, N., KOSTOVIC, I. & HOF, P. R. 2009. Annotation - Does Alzheimer's disease begin in the brainstem? *Neuropathol Appl Neurobiol.*, 35, 532-554.
- SIPOS, E., KURUNCZI, A., KASZA, Á., HORVATH, J., FELSZEGHY, K., LAROCHE, S., TOLDI, J., PARDUCZ, Á., PENKE, B. & PENKE, Z. 2007. Beta-Amyloid Pathology in the entorhinal cortex of rats induces memory deficits: Implications for Alzheimer's disease. *Neuroscience*, 147, 28-36.
- TANZI, R. E. & BERTRAM, L. 2005. Twenty Years of the Alzheimer's Disease Amyloid Hypothesis: A Genetic Perspective. *Cell*, 120, 545-555.
- TJERNBERG, L. O., NASLUND, J., LINDQVIST, F., JOHANSSON, J., KARLSTROM, A. R., THYBERG, J., TERENIUS, L. & NORDSTEDT, C. 1996. Arrest of beta-amyloid fibril formation by a pentapeptide ligand. *Journal of Biological Chemistry*, 271, 8545-8.
- TSIRULNIKOV, K., ABULADZE, N., BRAGIN, A., FAULL, K., CASCIO, D., DAMOISEAUX, R., SCHIBLER, M. J. & PUSHKIN, A. 2012. Inhibition of aminoacylase 3 protects rat brain cortex neuronal cells from the toxicity of 4-hydroxy-2-nonenal mercapturate and 4-hydroxy-2-nonenal. *Toxicology and Applied Pharmacology*, 263, 303-314.
- WANG, X. 2001. The expanding role of mitochondria in apoptosis. *Genes Dev*, 15, 2922-33.

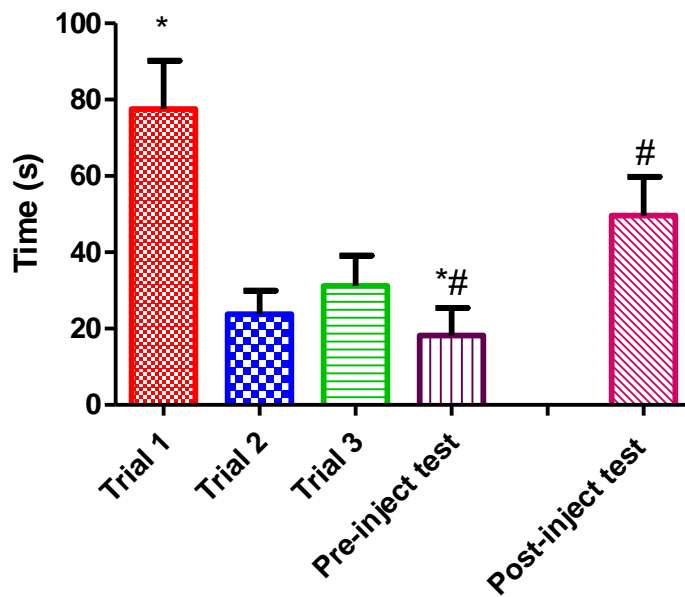
- WOLFER, D. P., MADANI, R., VALENTI, P. & LIPP, H.-P. 2001. Extended analysis of path data from mutant mice using the public domain software Wintrack. *Physiology & Behavior*, 73, 745-753.
- YAO, Z. X., DRIEU, K., SZWEDA, L. I. & PAPADOPOULOS, V. 1999. Free radicals and lipid peroxidation do not mediate beta-amyloid-induced neuronal cell death. *Brain Research*, 847, 203-10.
- ZENG, L., LI, T., XU, D. C., LIU, J., MAO, G., CUI, M. Z., FU, X. & XU, X. 2012. Death receptor 6 induces apoptosis not through type I or type II pathways, but via a unique mitochondria-dependent pathway by interacting with Bax protein. *J Biol Chem*, 287, 29125-33.
- ZHU, Z. H., WAN, H. T. & LI, J. H. 2011. Chuanxiongzine-astragaloside IV decreases IL-1beta and Caspase-3 gene expressions in rat brain damaged by cerebral ischemia/reperfusion: a study of real-time quantitative PCR assay. *Sheng Li Xue Bao*, 63, 272-80.

Appendix A

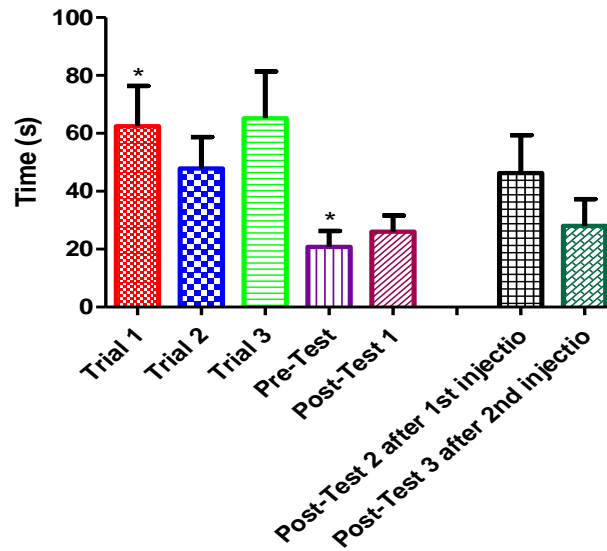
TB PRE & POST-INJECTION MWM RESULTS



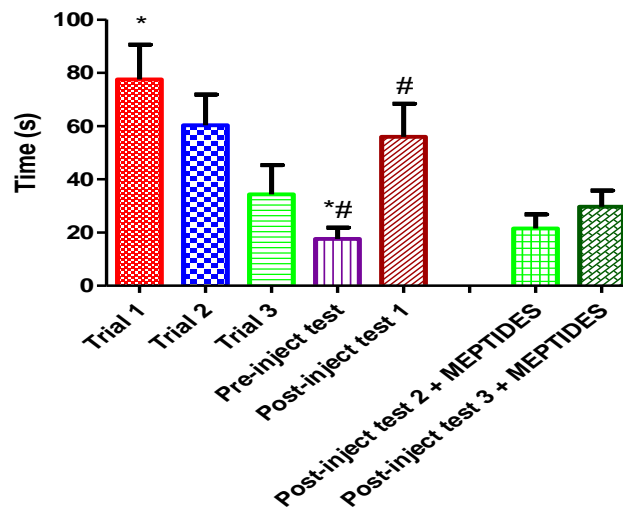
A β ₄₂ PRE & POST-LESION MWM RESULTS



TB+MEPTIDES PRE & POST-INJECTION MWM RESULTS

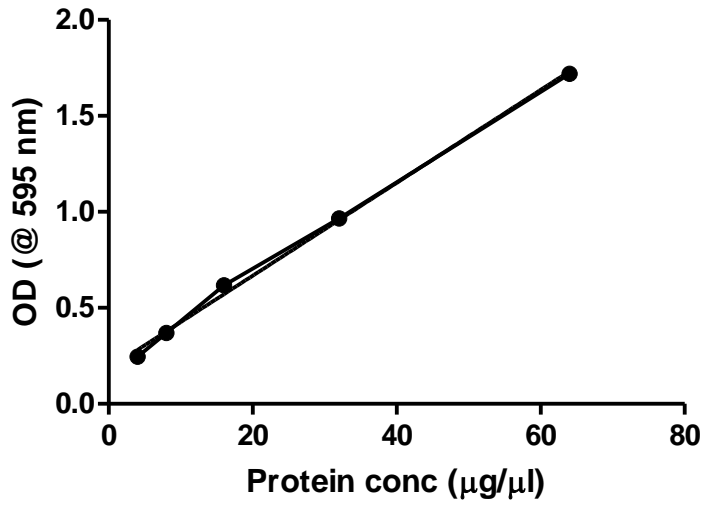


A β_{42} + MEPTIDE PRE & POST-INJECTION MWM RESULTS



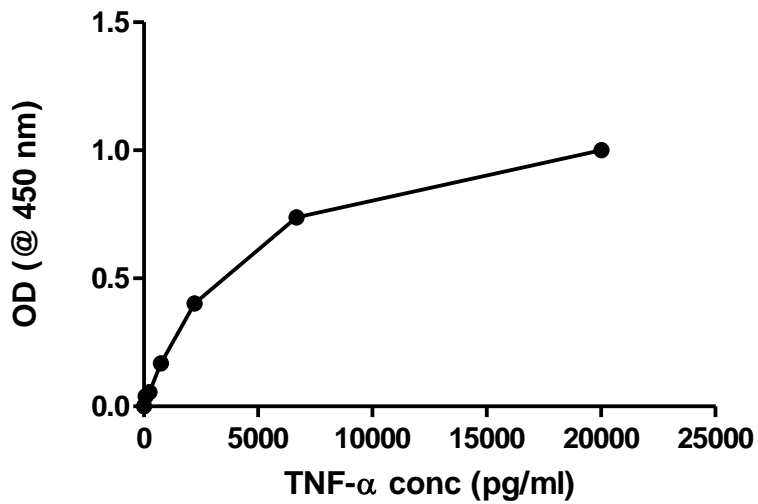
Graphs showing the pre- and post-injection MWM results of the TB, A β_{42} , TB + MEPTIDES and A β_{42} + MEPTIDES groups

WESTERN BLOT STANDARD CURVE



Graph showing Western blot standard curve. Standard samples OD range (0.221 – 1.901). Experimental tissue sample range (0.221 – 1.602).

TNF-Alpha ELISA STANDARD CURVE



Graph showing TNF-Alpha ELISA standard curve. Standard samples OD range (0.000 – 1.125). Experimental tissue sample range (0.393 – 0.518)

Appendix B

Western Blotting

Laemli Buffer system

Stock solutions

1. Acrylamide/Bis (30 %)
 - a. 87.6 g acrylamide (29.2 g/100 ml)
 - b. 2.4 g N'N'-bis-methylene-acrylamide (0.8 g/100 ml)

Make to 300 ml with distilled water. Filter and store at 4°C in dark. (Up to 30 days maximum)

2. 10 % SDS

Dissolve 10 g of SDS in 90 ml distilled water with gentle stirring and make up to 100 ml using deionised water.

3. 1.5 M Tris-HCl, pH 8.8

- a. 27.23 g Tris base (18.15 g/100 ml)
- b. 80 ml distilled water

Adjust pH to 8.8 with 6 N HCl. Bring total volume to 150 ml using distilled water after adjusting pH. Store at 4 °C.

4. 0.5 M Tris-HCl, pH 6.8

- a. 6 g Tris Base
- b. 60 ml distilled water

Adjust pH to 6.8 using 6N HCl. Bring total volume to 100 ml using distilled water after adjusting pH. Store at 4 °C.

5. 10 % APS (must be prepared fresh each time)

- a. 100 mg ammonium persulphate
- b. Dissolve in 1 ml distilled water

6. Sample Buffer (Stock)

- a. 3.55 ml distilled water
- b. 1.25 ml 0.5 Tris-HCl pH 6.8
- c. 2.5 ml glycerol
- d. 2 ml 10 % SDS

- e. 0.2 ml 0.5 % Bromophenol blue

Total volume 9.5 ml. Store at room temperature.

To use: Add 50 μ L β -mercaptoethanol to 950 μ l sample buffer prior to use. Dilute the sample at least 1:2 with sample buffer and heat at 95 °C for 4 minutes.

7. 10 x Running buffer (Stock)

- a. 30.3 g Tris base
- b. 144 g Glycine
- c. 10 g SDS

Dissolve and bring total volume up to 1000 ml (1 L) with distilled water. Do not adjust pH with acid or base. Store at 4 °C. If precipitation occurs warm to room temperature before use.

To use: Dilute 50 ml of the 10 x stock with 450 ml distilled water for each run. Mix thoroughly before use.

8. 10 x transfer buffer (Stock)

- a. 30.0 g Tris Base
- b. 144 g Glycine

Dissolve and bring total volume to 1 L with distilled water. Do not adjust pH with acid or base.

To use: Dilute 50 ml of the 10 x stock with 350 ml distilled water and 100 ml **methanol**. Mix thoroughly before use.

9. 10 x TBS

- a. 87.66 g Sodium chloride
- b. 12.11 g Tris
- c. 40 ml HCl

Make up to 1000 ml using distilled water. Adjust pH to 8.0. Note: 10 x TBS can be made in larger volumes and stored for long periods.

To use: Dilute 100 ml TBS in 900 ml distilled water and mix thoroughly.

10. 1 x TBS-T

Dilute 100 ml 10 x TBS in 900 ml distilled water and add 1 ml Tween 20. Mix thoroughly.

11. RIPA buffer

- a. 8.76 g NaCl
- b. 10 ml Tris pH 7.2 (1 M Tris)
- c. 10 ml 10 % SDS
- d. 1ml Triton X 100
- e. 10 g Na deoxycholate
- f. 10 ml 0.5 M EDTA

Make up to 1 L using distilled water and filter well before use. The buffer can be aliquoted in Eppendorf vials and stored at -20 °C.

12. Bradford's reagent (protein quantification)

- a. 50 mg Coomassie Brilliant Blue G250
- b. 50 ml methanol
- c. 100 ml 85 % Phosphoric acid
- d. 850 ml distilled water.

Dissolve 50 mg Coomassie brilliant Blue G250 in 50 ml methanol. To this add 100 ml phosphoric acid. Now add 500 ml distilled water. Filter and remove precipitates. Make up to 1 L using 350 ml distilled water.

Appendix C

Western Blotting (SDS PAGE)

Prepare gels (resolving gel and stacking gel) of required percentage.

Note: While allowing resolving gel to set, cover the surface with isobutanol

For 10 ml of resolving gel.

Percent Gel	Distilled H ₂ O (ml)	30% Acrylamide/Bis (ml)	1.5 M Tris pH 8.8 (ml)	10% SDS (ml)	10% APS (μ l)	TEMED (μ l)
4%	6.1	1.3	2.5	0.1	50	5
7%	5.1	2.3	2.5	0.1	50	5
10%	4.1	3.3	2.5	0.1	50	5
12%	3.4	4.0	2.5	0.1	50	5
14%	2.7	4.7	2.5	0.1	50	5
16%	2.1	5.3	2.5	0.1	50	5

Note: Add APS and TEMED immediately prior to pouring the gel

4% Stacking gel:

30% Acrylamide/Bis – 1.3 ml

0.5M Tris pH 6.8 – 2.5 ml

10% SDS – 100 μ l

Distilled water – 6 ml

10% APS – 100 μ l

TEMED – 10 μ l

Note: Adjust the volumes above accordingly to prepare different amounts of gels. Add APS and TEMED immediately prior to pouring the gel.

Electrophoresis

- Samples must be boiled at 95°C for 5 minutes prior to loading
- Assemble the electrophoresis apparatus and fill in 1x running buffer

- Load approx 5 μ l of the protein marker being used
- Load up to 25 μ l (20 μ g) protein in each well. (Note: Amount and volume of protein varies according to protein concentration, requirement and capacity of the wells)
- Run the gels at 200V (400 mA) for about 45 to 50 minutes or until the bottom most marker band runs to the bottom of the gels
- Equilibrate the gels in transfer buffer for about 10 mins

Transfer

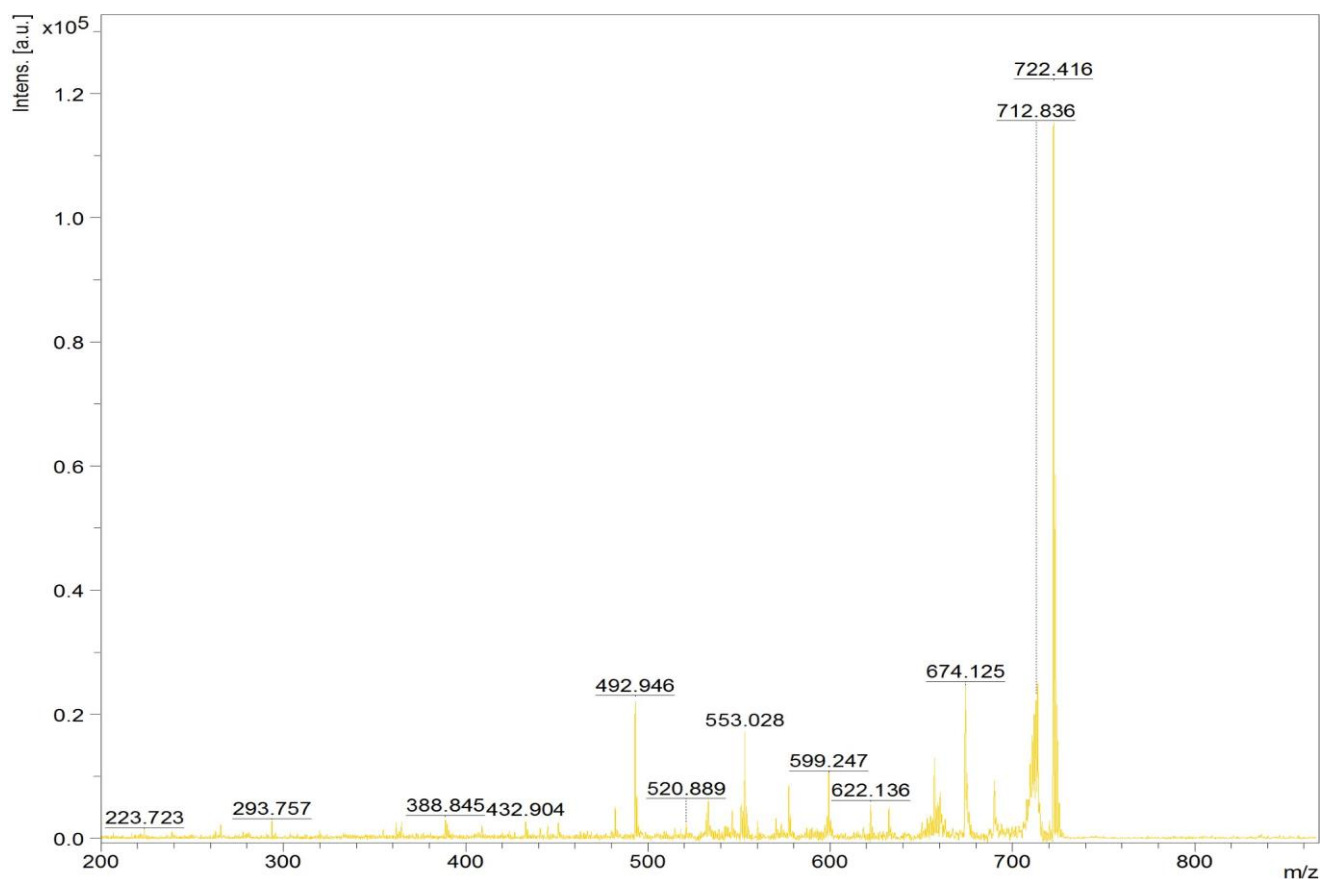
- Soak 2 pieces of extra thick (2.4 mm) filter paper per gel OR 6 pieces of thick filter paper (0.8 mm) per gel in transfer buffer
- If using nitrocellulose membrane, wet it in transfer buffer; if using a PVDF membrane, wet it in methanol or ethanol for 30 sec. Following this, wash the membranes for 1-2 mins in water and equilibrate in transfer buffer for 10 mins with agitation
- Assemble the sandwich for transfer on the cassette base: wet filter paper pieces at the bottom; membrane; the gel; the remaining wet filter paper pieces. Using the blot roller remove air bubbles
- Place the cassette lid over the base and secure the lid making sure the lid is tightly closed and electrical contacts fit closely into the slots in the base.
- Slide the cassette into the bay.
- Choose a standard SD protocol from the BioRad menu
- Initiate run by pressing the navigation button that corresponds to A: RUN for the upper bay and B: RUN for the lower bay.
- After run is complete place the membranes in methanol for about 30 seconds and dry on a tissue paper

Note: Always handle membranes using tweezers

Blocking

- The membrane is blocked in milk (5g fat free milk powder in 100 ml TBS-T). Prepare desired volume of milk. 25-30 ml is sufficient to immerse one membrane
- Block for 2 hours OR overnight

Appendix D



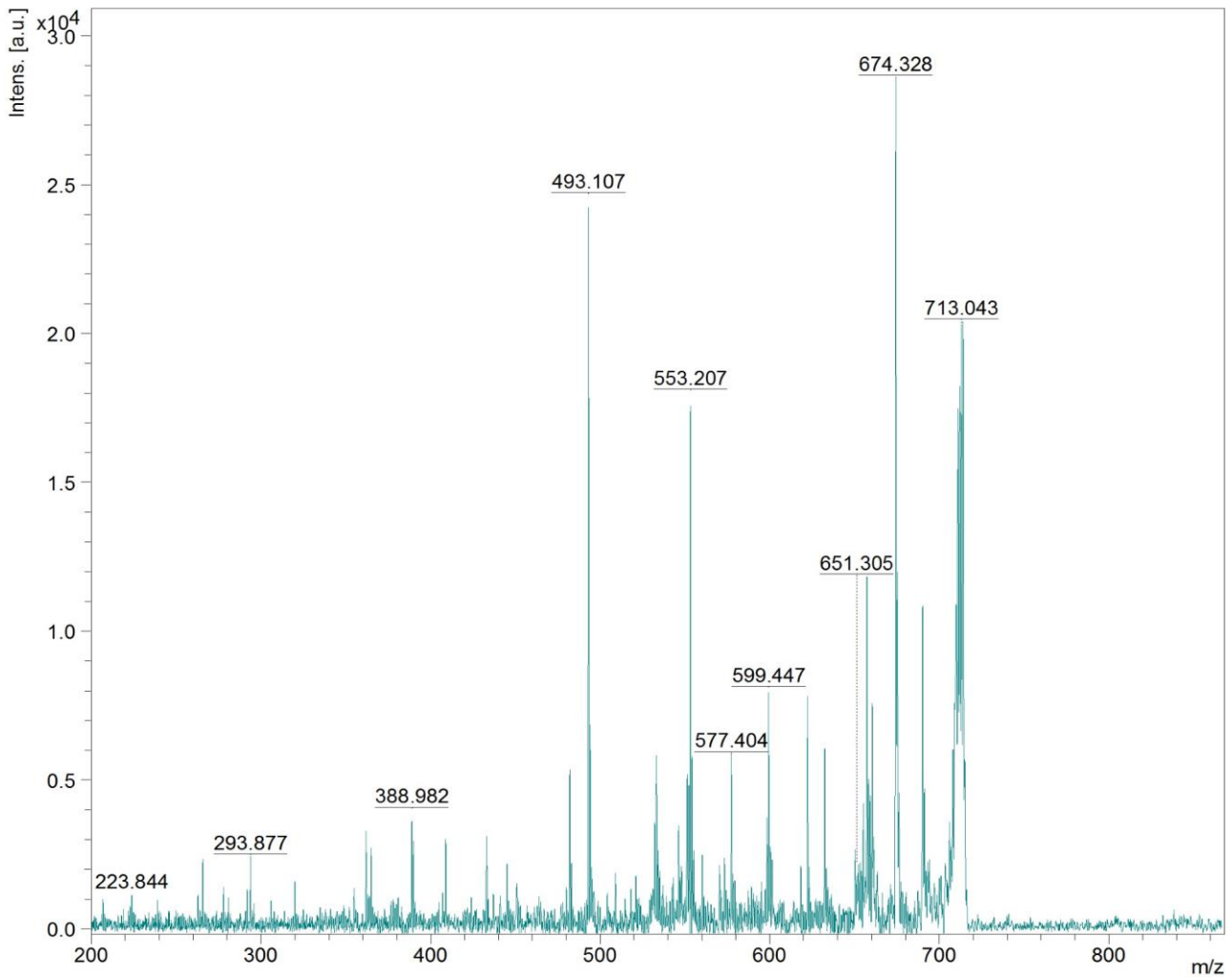
Date of acquisition 2014-07-15T17:18:24.644+00:00

Acquisition method name

Spectrum type	LIFT
Parent ion mass for ms/ms spectra	722.41
Precursor ion selector lower mass limit	4.696 Da
Precursor ion selector upper mass limit	4.696 Da
CID valve/mode	false 3000
Number of shots	

Bruker Daltonics flexAnalysis

Instrument Info	User	BDAL@DE
Instrument	FLEX-PC	
Instrument type	autoflexTOF/TOF	



Date of acquisition 2014-07-15T17:23:25.502+00:00

Acquisition method name

Spectrum type LIFT
Parent ion mass for ms/ms spectra 722.41
Precursor ion selector lower mass limit 4.696 Da
Precursor ion selector upper mass limit 4.696 Da
CID valve/mode false 2000
Number of shots

Instrument Info *User* BDAL@DE
Instrument FLEX-PC
Instrument type autoflexTOF/TOF